Spermatogonial kinetics in the human

Sara Di Persio[1], Rossana Saracino[1], Stefania Fera[1], Barbara Muciaccia[1], Valentina Esposito[1], Carla Boitani[1], Bartolomeo P. Berloco[2], Francesco Nudo[2], Gustavo Spadetta[3], Mario Stefanini[1], Dirk G. de Rooij[1,4,5], Elena Vicini[1,4,5]

[1] Fondazione Pasteur Cenci Bolognetti, Department of Anatomical, Histological, Forensic and Orthopaedic Sciences - Section of Histology and Medical Embryology, Sapienza University of Rome, Rome, 00161, Italy; [2] Department of General and Specialistic Surgery "Paride Stefanini", Sapienza University of Rome, Rome, 00161, Italy; [3] Department of Cardiovascular, Respiratory, Nephrological, Anesthesiological and Geriatric Sciences, Sapienza University of Rome, Rome, 00161, Italy

[4] Contributed equally to this study

[5] Corresponding authors:
Elena Vicini
Via Antonio Scarpa 14
00161 Roma, Italia
Tel +39 06 49766804
Fax + 39 06 4462 854
elena.vicini@uniroma1.it

[5] Dirk G. de Rooij
d.g.derooij@uu.nl

Summary Statement

Marker protein expression patterns allowed to better understand human spermatogonial development and stem cell renewal. Our new views on spermatogonial behavior will facilitate further research and solving fertility problems.

ABSTRACT

The human spermatogonial compartment is essential for daily production of millions of sperm. Despite this crucial role, the molecular signature, kinetic behavior and regulation of human spermatogonia are poorly understood. Using human testis biopsies with normal spermatogenesis and studying marker protein expression, for the first time we identified different subpopulations of spermatogonia. MAGE-A4 marks all spermatogonia, KIT marks all B spermatogonia and UCLH1 all Apale-dark (Ap-d) spermatogonia. We suggest that at the start of the spermatogenic lineage there are Ap-d spermatogonia that are GFRA1^{High} likely including the spermatogonial stem cells. Then UTF1 becomes expressed, cells become quiescent and GFRA1 expression decreases. Finally, GFRA1 expression is lost and subsequently cells differentiate into B spermatogonia, losing UTF1 and acquiring KIT expression. Strikingly, most of human Ap-d spermatogonia are out of cell cycle and even differentiating type B spermatogonial proliferation is restricted. A novel scheme for human spermatogonial development is proposed that will facilitate further research in this field, the understanding of cases of infertility and the development of methods to increase sperm output.

KEY WORDS: **Human, Spermatogonia, GFRA1, UTF1, KIT, UCL-H1, Stem Cell Renewal, Spermatogonial Differentiation**

INTRODUCTION

While extensive studies have rendered considerable knowledge on spermatogenesis in non-primate mammals, our understanding of this process in primates and especially in the human is still scanty. In both primates and non-primates, at the start of spermatogenesis there are so-called undifferentiated spermatogonia. In non-primates, this compartment consists of singles (A_s), pairs (A_{pr}) and chains (A_{al}) of spermatogonia. The spermatogonial stem cells (SSCs) are among the A_s spermatogonia (Aloisio et al., 2014; Chan et al., 2014; de Rooij and Russell, 2000; Helsel et al., 2017; Komai et al., 2014; Oatley et al., 2011). In primates, this compartment consists of Apale (Ap) and Adark (Ad) spermatogonia. The Ap spermatogonial nuclei stain lightly and evenly with hematoxylin and the Ad nuclei stain darkly and in the human show a non-staining rarefaction zone in the middle of the nucleus. Intriguingly, the Ad spermatogonia do not or rarely incorporate S phase markers as ^{3}H-thymidine or BrdU (Clermont, 1966a; Clermont, 1966b; Clermont, 1969; Clermont and Antar, 1973; Simorangkir et al., 2009) and are therefore considered to be quiescent. Several opinions exist as to the function of the Ap and Ad spermatogonia. One, the Ad spermatogonia are the ultimate stem cells that slowly produce Ap spermatogonia that would not have enough self-renewal capacity to maintain their numbers (Clermont, 1966a; Clermont, 1966b; Ehmcke et al., 2006). Two, the Ap spermatogonia are the SSCs as they produce differentiating spermatogonia, maintain themselves and produce quiescent Ad spermatogonia that in case of loss of Ap spermatogonia can convert into Ap spermatogonia again (Clermont, 1966a; Clermont, 1966b; Ehmcke and Schlatt, 2006; Hermann et al., 2010; van Alphen et al., 1988). Three, Ap and Ad are similar cells but in different phases of the cell cycle (Fouquet and Dadoune, 1986; Hermann et al., 2010; Hermann et al., 2009a).

In most monkey species and non-primate mammals, whole stretches of seminiferous tubules are in the same stage of the cycle of the seminiferous epithelium and subsequent stages follow each other along the length of the tubule. In contrast, in the human the epithelial stages occupy only small areas of the tubule basal lamina and neighboring areas are in randomly different epithelial stages (Johnson, 1994). The reason for this difference is supposed to be related to spermatogonial behavior.

Using testis material from human organ donors, we studied the proliferative activity and differentiation of human spermatogonial cell types to understand the seemingly large differences between human and non-primate spermatogenesis. The expression patterns of GFRA1, UCH-L1, KIT and UTF1 allowed us to distinguish spermatogonial subtypes and the expression of KI67 gave us information about the proliferative activity of these cell types. We established the clonal sizes of Ap and B spermatogonia and the number of generations of B spermatogonia. A novel concept of human spermatogonial proliferation is proposed. The new view on human spermatogonial behavior will greatly facilitate attempts to better understand abnormal spermatogenesis in male infertility patients.

RESULTS

Characterization of human spermatogonia

In rodents, great progress was made by characterizing spermatogonial cell types in whole mounts of seminiferous tubules stained with hematoxylin. Applying this technique to human seminiferous tubules, clearly recognizable Ap and Ad spermatogonia (Clermont, 1966b) were seen. However, often these cells had an intermediate morphology. For example, cells with nuclei staining lightly with hematoxylin as Ap, but having a nuclear rarefaction zone as in Ad spermatogonial nuclei (Fig. 1A). Especially in whole mounts, in which one always sees the whole nucleus, it is often too difficult to distinguish Ap and Ad spermatogonia, suggesting a gradual transition from Ap to Ad spermatogonia and/or vice versa. Also the morphological analysis of fluorescent-stained nuclei does not allow a clear distinction between Ap and Ad spermatogonia (Fig.1B). Because of this and because to date the specific function of Ap and Ad spermatogonia has remained unclear, we decided to no longer distinguish between Ap and Ad spermatogonia and to use the term Ap-d to indicate the total population of Ap and Ad spermatogonia. A further complication in spermatogonial recognition in the human is that specific fixation methods are required to distinguish B from Ap-d spermatogonia (Clermont, 1966b; Rowley and Heller, 1971).

Spermatogonial density on the basal lamina of human seminiferous tubules, is high. Solid packs of KIT^- Ap-d spermatogonia, of KIT^+ B spermatogonia or mixtures of these cell types can be seen (Fig. S1). Indeed, human spermatogonial density is

so high that the nuclei of the Sertoli cells moved to the second layer of cells above the basal lamina (Fig. S1). It proved to be impossible to discern individual clones of spermatogonia, connected by intercellular bridges, as in rodents (de Rooij, 1973; Huckins, 1971; Lok et al., 1982).

We decided to use marker proteins to distinguish human spermatogonial cell types. To identify Ap-d and B spermatogonia we used MAGE-A4, UCH-L1 and KIT. MAGE-A4 is expressed in all types of spermatogonia (Aubry et al., 2001), UCH-L1 is expressed in Ad-p spermatogonia (Tokunaga et al., 1999a; Tokunaga et al., 1999b) while KIT is specifically expressed in differentiating type spermatogonia (Schrans-Stassen et al., 1999). In prepubertal monkey testes that only contain Ap-d spermatogonia no KIT staining was found (Hermann et al., 2009b). Whole mounts of seminiferous tubules were immunofluorescently stained for MAGE-A4 and UCH-L1 (Fig. 1C) or MAGE-A4 and KIT (Fig. 1 E) UCH-L1 and KIT expression did not overlap, with only few spermatogonia weakly expressing UCHL-1 also weakly stained for KIT (Fig. 1G). Using these markers, UCH-L1^{+}/KIT^{-}/MAGE-A4^{+} cells represent the Ap-d and the UCH-L1^{-}/KIT^{+}/MAGE-A4^{+} cells represent the B spermatogonia. We found that 37 ± 4% of the MAGE-A4^{+} cells were KIT^{+} and therefore B and 63 ± 6% of the MAGE-A4 were UCH-L1^{+} and therefore, Ap-d spermatogonia (Fig. 1D,F). MAGE-A4 expression was weaker in B than in Ap-d and was absent in preleptotene spermatocytes (Fig. S2).

Expression of GFRA1 and UTF1 in Ap-d spermatogonia

We next analyzed expression of selected markers within the population of Ap-d by double or triple immunostaining for MAGE-A4 and/or UCH-L1. GFRA1 is a co-receptor for GDNF, a growth factor produced by Sertoli cells and peritubular cells (Singh et al., 2017; Spinnler et al., 2010) that regulates self-renewal and differentiation of murine SSCs and stimulates the proliferative activity of undifferentiated spermatogonia. GFRA1 is a consensus marker for early undifferentiated spermatogonia including SSCs (Meng et al., 2000) and is heterogeneously expressed in human Ad and Ap spermatogonia (Grisanti et al., 2009). KIT and GFRA1 double-staining revealed no double-positive cells (data not shown), indicating that B spermatogonia do not express GFRA1. By double immunostaining for MAGE-A4 and GFRA1 we found that GFRA1 is expressed in 54

± 8% of all spermatogonia (Fig. 2A,B) and in 87 ± 2% % of the Ap-d spermatogonia by double immunostaining for UCH-L1 and GFRA1(Fig. S3A).

UTF1 is a stably chromatin-associated, transcriptional repressor protein that is expressed in Ap-d spermatogonia (von Kopylow et al., 2010; von Kopylow et al., 2012). It is involved in the regulation of differentiation of ES and EC cells (Lin et al., 2012; van den Boom et al., 2007). UTF1 was expressed in 43 ± 3% (Fig. 2C,D) of total spermatogonia and in 56 ± 4% of the Ap-d spermatogonia (Fig. S3B). A few B spermatogonia weakly expressing KIT also weakly stained for UTF1 (Fig. 2E). We conclude that UTF1 is expressed in many Ap-d spermatogonia and only few B spermatogonia.

Since both GFRA1 and UTF1 are expressed in many Ap-d spermatogonia, this indicates that they are co-expressed in some Ap-d spermatogonia. In whole mounts stained for MAGE-A4, GFRA1 and UTF1 we found that 38 ± 5% of the spermatogonia were GFRA1^{+}, 17 ± 5% were UTF1+ and 25 ± 8% of the cells were double positive for GFRA1 and UTF1 (Fig. 2F,G). Similar results were obtained in whole mounts stained for UCH-L1, GFRA1 and UTF1 (Fig. S3C). Interestingly, we observed a clear difference in expression levels of GFRA1 in UTF1 positive and negative spermatogonia (Fig. 2F). Quantifying the fluorescence intensity of GFRA1 in the two subsets revealed that the level of GFRA1 in the GFRA^{+}/UTF1^{-} Ap-d was twice as high as in GFRA1^{+}/UTF1^{+} Ap-d spermatogonia (Fig. 2H).

Proliferative activity of human Ap-d spermatogonia

To learn about the proliferative activity of the Ap-d spermatogonia, we stained tubule whole mounts for KI67, a marker of cells in all phases of the cell cycle except G0 (Birner et al., 2001; Gerdes et al., 1984; Scholzen and Gerdes, 2000). In this experiment, MAGEA4^{+}/KI67^{+}/KIT^{-} spermatogonia represent Ap-d spermatogonia in active cell cycle. KI67^{+} Ap-d spermatogonia were singles, pairs as well as small groups of up to 6 cells (Fig. 3A). Only 5 ± 2% of the Ap-d spermatogonia appeared positive for KI67 (Fig. 3B) indicating that 95 ± 2% of the Ap-d spermatogonia are not in active cell cycle. Co-staining with MAGE-A4, GFRA1 and KI67 showed a comparable percentage of KI67^{+} Ap-d (6 ± 2%) strongly suggesting that GFRA1 expression captures all the Ap-d spermatogonia that are in active cell cycle (Fig. S4).

Interestingly, UTF1^{+} Ap-d spermatogonia never stained for KI67 or for EdU (data not shown) indicating that UTF1^{+} cells were quiescent. Therefore, all KI67^{+} Ap-d were GFRA1^{High}/UTF1^{-}. When only 6 % of the Ap-d spermatogonia are KI67^{+} it can be calculated that about 15 % of GFRA1+/UTF1^{-} (6% of 38%) are in active cell cycle.

These results suggest that early Ap-d spermatogonia are GFRA1 ^{High}/UTF1^{-} and that these cells slowly proliferate. When UTF1 becomes expressed these cells become quiescent and GFRA1 levels decrease.

Ap-d spermatogonia are mostly single cells and proliferate throughout the epithelial cycle

To study the topographical arrangement of Ap-d spermatogonia, we used the mitotic marker phosphohistone-H3 (PHH3) in whole mounted seminiferous tubules. Mitosis only takes a couple of hours and as clones of Ap-d spermatogonia are not synchronized with each other, at any given moment few Ap-d spermatogonia will be in mitosis, allowing one to observe clonal sizes despite the high spermatogonial density. Mitotic Ap-d spermatogonia (MAGE-A4^{+}/KIT^{-}/PHH3^{+}) were rare and were mostly single cells (74 ± 4%) and some pairs (26 ± 4%). The pairs may either be 2 single Ap-d spermatogonia that coincidentally entered mitosis simultaneously or a true pair of Ap-d spermatogonia connected by an intercellular bridge (Fig. 3C,D). No chains of mitotic Ap-d spermatogonia were observed. This indicates that in the human most, if not all, Ap-d spermatogonia are single cells. Apparently, human undifferentiated spermatogonia do not, or hardly, form pairs and chains of cells as frequently occurs in rodents. Therefore, it will be mostly single Ap-d spermatogonia that differentiate into B spermatogonia. Single KIT^{+}/PHH3^{+} cells, that should represent the division of the first generation of B spermatogonia, were observed. In response to the differentiation into B spermatogonia of some Ap-d, a comparable number of Ap-d spermatogonia should divide to replenish the cells lost to differentiation. Indeed, the number of dividing single KIT^{-}/PHH3^{+} Ap-d spermatogonia was comparable to that of single KIT^{+}/PHH3^{+} B spermatogonia (43 ± 7% versus 57 ± 7%, Fig. 3E).

We then asked whether divisions of Ap-d occur during particular stages of the epithelial cycle. In testis sections, mitotic spermatogonia were made clearly visible by immunofluorescent staining for PHH3 and for KIT, while epithelial stages were made

visible by acrosin co-staining (Muciaccia et al., 2014). Again, mitotic figures of the KIT^- Ap-d spermatogonia were rare (Fig. 3F). In samples from 6 donors, 64 KIT^- mitoses of Ap-d spermatogonia were found, spread throughout the epithelial stages although numbers tended to be highest during stage IX (Fig. 3G). Hence, Ap-d spermatogonia proliferate throughout the epithelial cycle.

Three generations of human differentiating type B spermatogonia

In mammals, successive generations of differentiating spermatogonia divide synchronously during specific stages of the epithelial cycle. Generally, the number of peaks of mitotic spermatogonia during the epithelial cycle equals the number of generations of differentiating spermatogonia. To reassess this number in the human, we used the 12-stage classification of the epithelial cycle (Muciaccia et al., 2013) and triple immunofluorescent staining of testis sections for acrosin to distinguish epithelial stages, for PHH3 to detect mitoses, and for KIT to detect B spermatogonia. In total, 260 KIT^+ mitoses were observed in sections of six donors (Fig. 4A). Clear peaks of mitotic activity of KIT^+ mitotic spermatogonia were found in epithelial stages IX, II/III and V/VI, indicating that in the human there are three generations of differentiating spermatogonia (Fig. 4B). As in primates differentiating spermatogonia are named B spermatogonia, these should be called B1, B2 and B3 spermatogonia, respectively. Our observations suggest that most, if not all, B spermatogonia are formed by differentiation of single Ap-d spermatogonia. When the B1 spermatogonia are singles, the B2 will be pairs and the B3 chains of 4 that will divide into chains of 8 preleptotene spermatocytes.

During spermatogenesis, germ cells in the differentiation pathway form clones of cells that after division remain connected by intercellular bridges and move through the cell cycle synchronously. We analyzed the topographical arrangement of clones of mitotic B spermatogonia in tubule whole mounts fluorescently stained for KIT and PHH3 (Fig. 4C). Mitotic clones of B1, B2 and B3 spermatogonia, were always found in groups ranging from 3 to 32 cells in which sometimes singles, pairs and larger clones could be distinguished (Fig. 4D). This indicates that relatively frequently, multiple clones of B spermatogonia synchronously traverse the cell cycle, causing them to enter mitosis simultaneously.

The regulation of human differentiating spermatogonial numbers

The number of three generations of B spermatogonia is higher than the one generation previously suggested by Clermont (Clermont, 1966b) but is still surprisingly low compared to the 5 to 6 generations of differentiating type spermatogonia observed in other mammals. We hypothesized that the number of human B spermatogonial divisions is downregulated, possibly because of the exceptionally high spermatogonial density. We therefore asked whether all B spermatogonia are in active cell cycle and analyzed the expression of KI67 (Fig. 5A). To our surprise, only 55 ± 10% of the B spermatogonia were KI67$^+$, suggesting that almost half of human B spermatogonia are out of cell cycle (Fig. 5B). Similar results were obtained using a different KI67 antibody (data not shown).

In rodents, all generations of differentiating spermatogonia are continuously proliferating. To verify that KI67 is a good spermatogonial proliferation marker we studied KI67 expression in mouse differentiating type spermatogonia. Examining long stretches of seminiferous tubules, KIT$^+$ spermatogonia negative for KI67 were never observed, confirming that in the mouse all differentiating spermatogonia are in active cell cycle (Fig. S5). This finding supports the validity of using KI67 expression to study the proliferative activity of human differentiating spermatogonia and our conclusion that a considerable number of human B spermatogonia is not in cell cycle. Apparently, the proliferation of human differentiating type spermatogonia is downregulated.

Furthermore, after each of the subsequent divisions, the number of B spermatogonia should double and consequently also the numbers of mitotic spermatogonia in the peaks. In contrast, the second mitotic peak is not higher than the first one and the third peak of mitotic B3 spermatogonia also does not seem to include twice the number of mitotic B2 spermatogonia. To study whether apoptosis could be the reason for the low numbers of mitotic B spermatogonia, we performed TUNEL staining to detect apoptotic cells. Indeed, apoptotic cells were detected on the basal lamina in between MAGE-A4$^+$ spermatogonia (Fig. 5C) and KIT$^+$ spermatogonia (Fig. 5D), making apoptosis a probable cause of the low peaks of mitotic B spermatogonia.

DISCUSSION

Viewing whole mounts of human seminiferous tubules, one sees a surprisingly high density of spermatogonia with a highly variable morphology making it impossible to distinguish spermatogonial subtypes. However, immunofluorescent staining for GFRA1, UCH-L1, UTF1 and KIT allowed to discern sequential subpopulations of Ap-d spermatogonia. Furthermore, the regulation of B spermatogonial proliferation appeared to be more elaborate than in other mammalian species. The results led to the development of a novel model for steady state kinetics of human spermatogonia.

It proved impossible to reliably subdivide undifferentiated spermatogonia into Ap and Ad spermatogonia in tubule whole mounts, too many cells have an in between morphology suggesting a gradual transition from Ap to Ad. In monkey spermatogenesis too, cells intermediate between Ap and Ad have been described and these were called A-transition (At) (Fouquet and Dadoune, 1986) or A-unclassified (Aunc) (Simorangkir et al., 2005). Furthermore, Ehmcke and Schlatt reported that in primates 25 to 50% of the A spermatogonia cannot be unequivocally characterized as Ap or Ad (Ehmcke and Schlatt, 2006). We decided not to subdivide Ap-d spermatogonia on basis of their nuclear morphology but on the expression of marker proteins.

Our results show that all human spermatogonial cell types express MAGE-A4 and that 37% of the spermatogonia express KIT and are therefore B spermatogonia. The remaining KIT- spermatogonia are Ap-d spermatogonia that stain for UCHL1 with a small overlap of cells staining weakly for UCLH1 and KIT that are likely in transition between Ap-d and B (Fig. 6).

In line with our previous results, most Ap-d spermatogonia express the GDNF receptor GFRA1 (Grisanti et al., 2009) (Fig. 6). In this, human Ap-d spermatogonia resemble those of the rhesus monkey in which all Ap-d spermatogonia express GFRA1 (Hermann et al., 2009b). Only 6% of the $GFRA1^+$ Ap-d spermatogonia also express KI67, indicating that most of these cells are not in cell cycle. The transcription factor UTF1 is also expressed in a majority 56 ± 4% of Ap-d and in very few B spermatogonia. UTF1 has been associated with the capacity of human embryonal carcinoma cells to differentiate in response to RA (Lin et al., 2012). Interestingly, in rodents the differentiation of A_{al} spermatogonia into differentiating type spermatogonia is induced by RA. A few $UTF1^+$ B spermatogonia weakly

express UTF1 and also weakly express KIT. In view of the suggested role of UTF1 in RA action, it seems likely that the UTF1 weak B spermatogonia are in the process of losing UTF1 and acquiring KIT expression during the differentiation of Ap-d into B spermatogonia. Remarkably, UTF1 $^{+}$ spermatogonia never co-stain for KI67 indicating that UTF1 expressing Ap-d spermatogonia are quiescent. All proliferative activity in the compartment of Ap-d spermatogonia is therefore carried out by GFRA1^{+}/UTF1^{-} cells. Interestingly, the expression level of GFRA1 in GFRA1^{+}/UTF1^{-} Ap-d is 2-fold higher than in GFRA1^{+}/UTF1^{+} Ap-d spermatogonia. This indicates that the acquisition of UTF1 expression is an important step in the development of Ap-d spermatogonia as they become both quiescent and GFRA1^{Low}.

Based on our results, we suggest the following picture for the human spermatogonial compartment. At the start of the human spermatogenic lineage, there is a pool of GFRA1^{High}/UTF1^{-} Ap-d, comprising 32% of all Ap-d spermatogonia, which in the normal epithelium slowly proliferate (Fig. 6). Each epithelial cycle, some cells in the GFRA1^{+}/UTF1^{-} pool start to express UTF1 and become part of a pool of quiescent UTF1^{+}/GFRA1^{Low} Ap-d, comprising 56% of all Ap-d spermatogonia. At some moment, GFRA1 expression is lost and the cells become part of a compartment of GFRA1-/UTF1+ spermatogonia that may be competent to differentiate into B1 spermatogonia as evidenced by the occurrence of cells weakly stained for both UTF1 and the differentiation marker KIT (Fig. 6). In contrast to UTF1, UCH-L1 is expressed in all Ap-d spermatogonia and similarly to UTF1, UCH-L1 expression is lost in B spermatogonia. Recently, a single cell RNA seq experiment was carried out on human spermatogonia (Neuhaus et al., 2017). Heterogeneous expression profiles were found but the results did not yet lead to a better insight into spermatogonial behavior in the human. However, when the results can be related to our initial scheme based on GFRA1, UTF1 and KIT expression, the single cell RNA seq approach may well lead to a further refinement of our proposed scheme. Our data obtained using the marker PHH3 that labels the relatively rare mitotic Ap-d spermatogonia in whole mounts of seminiferous tubules, show that at least the majority of human Ap-d spermatogonia are single cells. Some pairs of Ap-d spermatogonia were also found but we do not know whether these are true pairs or mitotic singles that happen to be in each other neighborhood. Comparable numbers of single mitotic Ap-d spermatogonia were found as single mitotic B spermatogonia.

Apparently, single Ap-d spermatogonia differentiate into single B spermatogonia that subsequently enter the cell cycle and comparable numbers of single Ap-d spermatogonia divide to replenish the Ap-d spermatogonia lost to differentiation.

During the human epithelial cycle, there are three peaks of mitotic activity of B spermatogonia indicating the presence of three generations of B spermatogonia, B1, B2 and B3. The B1 spermatogonia being single cells and probably some pairs, this means that the spermatocytes consist of clones of 8 to 16 cells compared to about 1000 in mice (Russell et al., 1990). This difference will be smaller in monkeys in which 4-5 spermatogonial divisions have been found (Clermont and Antar, 1973; de Rooij and Russell, 2000; Ehmcke et al., 2005; Fouquet and Dadoune, 1986). We found three generations of B spermatogonia and not one generation as previously described (Clermont, 1966b). In our analysis we used the novel 12-stage classification and not the 6-stage classification of the human epithelial cycle used by Clermont (Muciaccia et al., 2013). The shorter duration of each stage in the novel classification, allowed a more detailed analysis of mitotic peaks.

Only few of the GFRA1^{High}/UTF1^{-} Ap-d spermatogonia stain for KI67 and are therefore in active cell cycle. This begs the question: “how much proliferative activity is needed to replenish the Ap-d lost to differentiation”? Using our data we can give a possible answer. During the steady state, once every epithelial cycle, B1 spermatogonia should be formed by differentiation of Ap-d spermatogonia. We showed that 37 out of every 100 spermatogonia are B spermatogonia. When there is no apoptosis of B spermatogonia, one seventh of these cells (about 5 spermatogonia) should be B1 spermatogonia (1B1 – 2B2 – 4B3, so B1 spermatogonia compose 1/7th of the total). We also found that only 15 out of every 100 GFRA1^{High}/UTF1^{-} Ap-d spermatogonia are in active cell cycle. Therefore, during the steady state, about 5 out of 15 (1/3rd) GFRA1^{High}/UTF1^{-} Ap-d spermatogonia, should divide once during one epithelial cycle to replenish Ap-d spermatogonia lost to differentiation. This suggests that on average the GFRA1^{High}/UTF1^{-} Ap-d only divide once every 3 epithelial cycles, i.e. one and a half months, and that these cells are out of the cell cycle for prolonged periods of time. In comparison, in rodents and the ram, $A_{s,pr,al}$ spermatogonia divide two to three times per epithelial cycle (Lok and de Rooij, 1983; Lok et al., 1983; Tegelenbosch and de Rooij, 1993). Furthermore, as indicated above in this calculation 5 UTF1^{+} Ap-d become B spermatogonia which is

7% of UTF1^{+} Ap-d spermatogonia, should be recruited for differentiation each epithelial cycle. This suggests that per epithelial cycle, UTF1^{+} Ap-d only have a chance of about 7% to leave the pool of quiescent Ap-d spermatogonia. Therefore, each epithelial cycle only a small proportion of the Ap-d can make the step to differentiating type spermatogonia and therefore, on average, the UTF1^{+} cells may stay quiescent for about 7-8 months.

It is conceivable that the long periods of time during which both GFRA1^{HIGH}/UTF1^{-} and GFRA1^{Low}/UTF1^{+} Ap-d spermatogonia are not in cell cycle brings along a gradual transition from the Ap to the Ad morphology. When this is indeed the case for both these cell types, the distinction between Ap and Ad spermatogonia clearly does not relate to different cell types and the latter would explain why over time little progress has been made in understanding primate spermatogonial behavior. Nuclear rarefaction zones as seen in typical Ad spermatogonia, have also been described in undifferentiated spermatogonia in mice and the Chinese hamster and were found to be to restricted to cells in G0/G1 phase (de Rooij, 1973; Lok et al., 1982). Nothing can be said as yet about whether or not the acquisition of the Ad morphology influences the chance of GFRA1^{High}/UTF1^{-} cells to enter the cell cycle or the responsiveness of the GFRA1^{Low}/UTF1^{+} cells to a differentiation stimulus. In rodents, the chains of A-aligned spermatogonia become quiescent at about stage II at which point they become capable to respond to induction of differentiation by retinoic acid (Endo et al., 2015). Therefore, quiescence of the cells may be related to competence of the cells towards induction of differentiation and UTF1 may be involved in inducing quiescence of these cells.

While in the mouse, all differentiating type spermatogonia express KI67, only 55% of human B spermatogonia did so. This indicates that at any given moment almost half of human B spermatogonia are not in active cell cycle. This may occur in two ways. One, B spermatogonia have a low random chance to enter the cell cycle, or two, they are inhibited to proliferate during particular time periods of the epithelial cycle. The first possibility does not seem attractive as it does not explain the occurrence of only 3 mitotic peaks, in fact one would not even expect the presence of peaks. The second option offers the possibility for the epithelium to restrict the number of B spermatogonial divisions by inducing quiescence of these cells during particular epithelial stages. Such a regulatory pathway governing the number of

differentiating spermatogonial generations, will have to be confirmed in further studies. In rodents, differentiating spermatogonia are always in active cell cycle. Apparently, in the human and possibly in other primates where generally about 4-5 generations of B spermatogonia are described there is a mechanism to control the number of generations of differentiating type spermatogonia.

In addition, there may be density related apoptosis of B spermatogonia that causes a reduction of B spermatogonial mitoses during the second and third mitotic peaks. Indeed, as assessed by TUNEL staining, spermatogonial apoptosis does take place. Apoptosis of differentiating type spermatogonia is observed in all non-primate mammals and serves to regulate cell density. In areas with many differentiating spermatogonia many of these cells will enter apoptosis and in areas with only few of these cells few or none will do so. This ensures an even distribution of preleptotene spermatocytes over the tubule basal lamina (de Rooij and Janssen, 1987; de Rooij and Lok, 1987).

In the human and some monkeys (Wistuba et al., 2003), areas that are in the same epithelial stage are only small, leading to the presence of multiple stages in one tubule cross-section. Our data supply several reasons for this phenomenon to occur. In humans, only singles and perhaps a few pairs of Ap-d differentiate, instead of the chains of 4 to 16 A_{al} spermatogonia in rodents. Furthermore, in the human there are fewer generations of differentiating spermatogonia to follow than in rodents, i.e. three instead of six, making a further 8-fold difference. Both reasons will lead to much smaller tubule areas being in the same epithelial stage in the human than in rodents.

Thus far, both Ap and Ad were considered stem cells. Our results suggest that the SSCs will reside in the population of the Ap-d spermatogonia that are GFRA1^{High}/UTF1^{-}. However, one has to be wary to assign a stem cell role to all of these cells as in the mouse it has recently been shown that only some of the single As spermatogonia are ultimate stem cells while the rest of the singles likely have a limited self-renewal capacity (Aloisio et al., 2014; Chan et al., 2014; Helsel et al., 2017; Komai et al., 2014; Oatley et al., 2011). Interestingly, mouse ultimate SSCs have recently been found to be GFRA1^{High} (Helsel et al., 2017) suggesting that in the human too the 32% Ap-d spermatogonia that are GFRA1^{High}/UTF1^{-} are, or at least, include the SSCs. This will need further studies.

In conclusion, GFRA1 and UTF1 are marker proteins enabling one to subdivide the human spermatogonial compartment in a more meaningful way than by using nuclear morphology. We suggest that the development of Ap-d spermatogonia can be subdivided into 3 steps: The earliest Ap-d spermatogonia that are GFRA1^{High} and include SSCs, then the Ap-d spermatogonia that start to express UTF1, their GFRA1 expression decreases and the cells become quiescent and finally GFRA1 expression stops and the cells become competent to differentiate into B spermatogonia (Fig. 6). The study of additional markers may well add further details to this process of Ap-d development and SSC renewal. Furthermore, our results will be particularly helpful in the interpretation of single RNA seq data. Also, it will facilitate the understanding of cases of male infertility due to spermatogonial failure and help the development of treatment strategies. In this respect, when UTF1^{+} Ap-d are analogous to A_{al} spermatogonia, it is interesting that the latter cells can be induced to differentiate already in stages II to VI by injection of retinoic acid (Endo et al., 2015).

MATERIALS AND METHODS

Human testis sample collection

Testicular biopsies were used from heart-beating organ donors (n= 15 samples from 19 to 75 years of age) at the hospital Policlinico Umberto I in Rome. For each donor, the free and informed consent of the family concerned, was obtained. The Ethical Committee of the hospital approved the use of human material according to national guidelines for organ donation as issued by the Italian Ministry of Public Health. Biopsies were collected as previously described (Muciaccia et al., 2013). From each donor, representative samples from different parts of the testis were collected. After collection the biopsies were transported in cold phosphate buffered saline (PBS) (Sigma-Aldrich, Milan, Italy) to the laboratory and processed within one hour. Biopsies were routinely fixed in Bouin's fixative and embedded in paraffin but in some instances samples were fixed in 10% buffered formalin (Sigma-Aldrich, Milan, Italy) or 4% paraformaldehyde (PFA) (Electron Microscopy Sciences, Hatfield, PA, USA). Some biopsies were left unfixed and used for short-term culture.

In order to check the integrity of the tissue and the preservation of spermatogenesis, Bouin-fixed samples were paraffin-embedded and sections stained with Mayer's hematoxylin and Eosin (Sigma-Aldrich, Milan, Italy) and analyzed. All the samples included in this study shown a well preserved testicular tissue and a normal spermatogenesis without any sign of fibrosis or inflammation.

EdU incorporation and detection

Unfixed testicular fragments obtained from biopsies were cultured in αMEM medium containing 4 mM glutamine,1% non essential amino acids, 2% penicillin / streptomycin, 0,08 % gentamicin, 15 mM Hepes pH 7.7 and 10μM EdU (5-ethynyl-2´-deoxyuridine) at 34 °C in 5% CO2 for 2 hours and 30 minutes (all reagents from: Thermo Fisher Scientific, Waltham, MA, 02451 USA). After incubation, fragments were gently disembroiled to obtain isolated seminiferous tubules and fixed in 4% paraformaldehyde at 4°C for 4 hours. EdU detection was performed following the protocol of the Click-iT EdU Imaging Kits (Thermo Fisher Scientific). Following EdU detection, tubules were used to detect various antigens using whole mount immunofluorescence.

Immunofluorescence

Five μm-thick sections of formalin-fixed samples were processed in a microwave oven for antigen retrieval in 6.0 pH citrate buffer (DAKO, Milan, Italy). To reduce unspecific background signal, sections were incubated with 1M glycine (Sigma-Aldrich, Milan, Italy) and subsequently with 1% BSA (Sigma-Aldrich, Milan, Italy) and 5% Normal Donkey Serum (Jackson Laboratories Immuno Research Europe Ltd, Newmarket, UK). Subsequently, sections were incubated overnight at 4°C with appropriate primary antibodies. The primary antibodies employed are listed in Table S1. After the washes, the sections were incubated with species specific secondary antibodies, for 2 hours at room temperature. All secondary ALEXA488-, Cy3-conjugated antibodies were from Jackson Immuno Research Europe Ltd (Newmarket, UK). At the end, the nuclei were counterstained with TO-PRO-3 Iodide (642/661) (T3605 Thermo Fisher Scientific, Waltham, MA, 02451 USA) and the slides closed with Vectashield mounting medium (Vector Laboratories, Inc.

Burlingame, CA, 94010 USA). Pictures were acquired using a Leica TCS SP2 confocal microscope with 40x oil immersion objective.

For whole mount immunofluorescence, seminiferous tubules were disentangled from testicular biopsies and immediately fixed in 4% PFA at 4°C for 4 hours. Fixed tubules were permeabilized with 0,5% Triton X100, treated with Glycine 1M for 1 hour ,and with 0.1%Triton X-100, 1%BSA, 5% Normal Donkey Serum in PBS overnight at 4°C. The following day, tubules were washed in 1%BSA 0.1% Triton X-100 in PBS (3 times for 30 minutes) and incubated overnight at 4°C with appropriate primary antibodies (Table S1).

The following day tubules were washed as above and incubated with species-specific secondary antibodies conjugated to ALEXA488, Cy3 or Cy5 fluorochromes, for 2 hours at room temperature. Primary and secondary antibodies were diluted in 1%BSA 0,1% Triton X-100 in PBS. After the secondary antibody, tubule were washed as above and nuclei were stained with TO-PRO-3. Tubules were mounted on slides with Vectashield mounting medium and observed with a Leica TCS SP2 confocal microscope with 40x oil immersion objective or an inverted Olympus IX83 microscope with 60X water immersion objective.

Whole-mount immunofluorescence analysis of adult mouse seminiferous tubules was performed as previously described (Corallini et al., 2006). Fixed seminiferous tubules were incubated with primary antibodies (Table S1) at 4°C for 16 h under constant shaking. After washing, the tubules were incubated with the species-specific conjugated secondary antibodies for two hours at room temperature. Nuclei were stained with TO-PRO-3.

For quantification of GFRA1 expression levels, intact seminiferous tubules from three different testis samples were co-stained for GFRA1 and UTF1. Z-stacks were acquired using Leica TCS SP2 confocal microscope at 1µm increments between z-slices with 40x oil immersion objective. All images were taken under the same conditions. The mean fluorescence intensity was quantified using LAS AF Software. For each donor, 80 cells were selected and analyzed from several seminiferous tubules.

TUNEL assay

The TUNEL (TdT-mediated X-dUTP nick end labeling) assay on human intact seminiferous tubules was performed as previously described (Hamer et al., 2003)

using the In Situ Cell Death Detection Kit, Fluorescein (Roche Diagnostic, Monza, Italy) with minor modifications. The PFA-fixed tubules were permeabilised with 1% Triton X-100 (Sigma-Aldrich, Milan, Italy) for 1 hour at room temperature. After two washes in PBS some tubules were treated with RNase-Free DNase Set (Qiagen, Milan, Italy) for 20 minutes at room temperature as positive control. Tubules were then briefly washed in PBS and incubated in TUNEL mix (enzyme plus label) at 37°C for 2 hours. As negative control, some tubules were incubated only with the TUNEL label (without enzyme) at 37°C for 2 hours. At the end, tubules were washed three times with PBS and they were used for detection of different antigens using whole mount immunofluorescence.

Imaging and spermatogonial quantification

In order to quantify the relative proportion of Ap-d subsets and the proliferation index of Ap-d and B spermatogonia, intact seminiferous tubules from at least three different testis samples were co-stained for relevant antibodies. Due to the convoluted nature of human seminiferous tubules, in order to image the entire spermatogonial layer, Z-stacks were acquired using Leica TCS SP2 confocal microscope with 40x oil immersion objective or an inverted Olympus IX83 microscope with 60X water immersion objective. For each testis sample, ten fields (187.5 x 187.5 µm) were randomly selected from at least three different seminiferous tubules. For each field, confocal z-stacks were acquired (at 1µm increments between z-slices).

To estimate the size and the frequency of $PHH3^+/KIT^+$ groups, five different samples were used. In each sample, stained tubules were individually analyzed from the beginning to the end in order to detect $PHH3^+/KIT^+$ cells. Z-stacks (at 1µm increments between z-slices) were then acquired for each field containing labeled cells.

In order to estimate the frequency of mitotic Ap-d and B spermatogonia, testis sections from six samples were co-stained for relevant antibodies and analyzed using Leica TCS SP2 confocal microscope with 40x oil immersion objective. $PHH3^+$ spermatogonia were rare and therefore several sections from each sample had to be analyzed to reach an adequate number of observations.

All quantifications were performed on stored microphotographs using the LAS AF Software or Fiji/ImageJ Software.

Statistical analysis

All quantitative data are shown as the mean ± standard error of the mean (SEM). To define the significance of the differences between two groups, data were analyzed using a t-test. To compare many groups, data were analyzed using a one-way analysis of variance (ANOVA) followed by a post hoc Fisher LSD Method. The significance level was fixed at $\alpha = 0.05$.

Acknowledgements

We are grateful to Stefania De Grossi and Tiziana Menna for excellent technical support and Dr. G. Spagnoli (Basel, Switzerland) for kindly providing the mouse anti-MAGE-A4 antibody. We acknowledge the Centre for Life Nano Science of the Istituto Italiano di Tecnologia for providing microscopy facilities and we would like to thank Dr. S. De Panfilis for assistance in using the instruments. This work was supported by grants from Sapienza University (Ateneo 2014- 2016) and from Fondazione Pasteur-Cenci Bolognetti to E.V.

Competing interests

The authors declare no competing or financial interests.

Author contributions

S.D.P., D.G.d.R., E.V. designed research; S.D.P., R.S., B.M., S.F., V.E., C.B., M.S. and E.V. performed research; B.P.B., F.N., G.S., provided human samples; S.D.P., M.S., D.G.d.R. and E.V. analyzed data; S.D.P., D.G.d.R., E.V. wrote the paper.

REFERENCES

Aloisio, G. M., Nakada, Y., Saatcioglu, H. D., Pena, C. G., Baker, M. D., Tarnawa, E. D., Mukherjee, J., Manjunath, H., Bugde, A., Sengupta, A. L., et al. (2014). PAX7 expression defines germline stem cells in the adult testis. *J. Clin. Invest.* **124**, 3929-3944.

Aubry, F., Satie, A. P., Rioux-Leclercq, N., Rajpert-De Meyts, E., Spagnoli, G. C., Chomez, P., De Backer, O., Jegou, B. and Samson, M. (2001). MAGE-A4, a germ cell specific marker, is expressed differentially in testicular tumors. *Cancer* **92**, 2778-2785.

Birner, P., Ritzi, M., Musahl, C., Knippers, R., Gerdes, J., Voigtländer, T., Budka, H. and Hainfellner, J. A. (2001). Immunohistochemical detection of cell growth fraction in formalin-fixed and paraffin-embedded murine tissue. *Am. J. Pathol.* **158**, 1991-1996.

Chan, F., Oatley, M. J., Kaucher, A. V., Yang, Q. E., Bieberich, C. J., Shashikant, C. S. and Oatley, J. M. (2014). Functional and molecular features of the Id4+ germline stem cell population in mouse testes. *Genes Dev.* **28**, 1351-1362.

Clermont, Y. (1966a). Renewal of spermatogonia in man. *Am. J. Anat.* **118**, 509-524.

---- (1966b). Spermatogenesis in man. A study of the spermatogonial population. *Fertil. Steril.* **17**, 705-721.

---- (1969). Two classes of spermatogonial stem cells in the monkey (Cercopithecus aethiops). *Am. J. Anat.* **126**, 57-71.

Clermont, Y. and Antar, M. (1973). Duration of the cycle of the seminiferous epithelium and the spermatogonial renewal in the monkey Macaca arctoides. *Am. J. Anat.* **136**, 153-165.

Corallini, S., Fera, S., Grisanti, L., Falciatori, I., Muciaccia, B., Stefanini, M. and Vicini, E. (2006). Expression of the adaptor protein m-Numb in mouse male germ cells. *Reproduction* **132**, 887-897.

de Rooij, D. G. (1973). Spermatogonial stem cell renewal in the mouse. I. Normal situation. *Cell Tissue Kinet.* **6**, 281-287.

de Rooij, D. G. and Janssen, J. M. (1987). Regulation of the density of spermatogonia in the seminiferous epithelium of the Chinese hamster: I. Undifferentiated spermatogonia. *Anat. Rec.* **217**, 124-130.

de Rooij, D. G. and Lok, D. (1987). Regulation of the density of spermatogonia in the seminiferous epithelium of the Chinese hamster: II. Differentiating spermatogonia. *Anat. Rec.* **217**, 131-136.

de Rooij, D. G. and Russell, L. D. (2000). All you wanted to know about spermatogonia but were afraid to ask. *J. Androl.* **21**, 776-798.

Ehmcke, J., Luetjens, C. M. and Schlatt, S. (2005). Clonal organization of proliferating spermatogonial stem cells in adult males of two species of non-human primates, Macaca mulatta and Callithrix jacchus. *Biol. Reprod.* **72**, 293-300.

Ehmcke, J. and Schlatt, S. (2006). A revised model for spermatogonial expansion in man: lessons from non-human primates. *Reproduction* **132**, 673-680.

Ehmcke, J., Wistuba, J. and Schlatt, S. (2006). Spermatogonial stem cells: questions, models and perspectives. *Hum. Reprod. Update* **12**, 275-282.

Endo, T., Romer, K. A., Anderson, E. L., Baltus, A. E., de Rooij, D. G. and Page, D. C. (2015). Periodic retinoic acid-STRA8 signaling intersects with periodic germ-cell competencies to regulate spermatogenesis. *Proc. Natl. Acad. Sci. U.S.A.* **112**, E2347-2356.

Fouquet, J. P. and Dadoune, J. P. (1986). Renewal of Spermatogonia in the Monkey (Macaca-Fascilularis). *Biol. Reprod.* **35**, 199-207.

Gerdes, J., Lemke, H., Baisch, H., Wacker, H. H., Schwab, U. and H., S. (1984). Cell cycle analysis of a cell proliferation-associated human nuclear antigen defined by the monoclonal antibody Ki-67. *I. Immunol.* **133**, 1710-1715.

Grisanti, L., Falciatori, I., Grasso, M., Dovere, L., Fera, S., Muciaccia, B., Fuso, A., Berno, V., Boitani, C., Stefanini, M., et al. (2009). Identification of spermatogonial stem cell subsets by morphological analysis and prospective isolation. *Stem Cells* **27**, 3043-3052.

Hamer, G., Roepers-Gajadien, H. L., Gademan, I. S., Kal, H. B. and De Rooij, D. G. (2003). Intercellular bridges and apoptosis in clones of male germ cells. *Int J Androl* **26**, 348-353.

Helsel, A. R., Yang, Q. E., Oatley, M. J., Lord, T., Sablitzky, F. and Oatley, J. M. (2017). ID4 levels dictate the stem cell state in mouse spermatogonia. *Development* **144**, 624-634.

Hermann, B. P., Sukhwani, M., Hansel, M. C. and Orwig, K. E. (2010). Spermatogonial stem cells in higher primates: are there differences from those in rodents? *Reproduction* **139**, 479-493.

Hermann, B. P., Sukhwani, M., Simorangkir, D. R., Chu, T., Plant, T. M. and Orwig, K. E. (2009a). Molecular dissection of the male germ cell lineage identifies putative spermatogonial stem cells in rhesus macaques. *Hum Reprod* **24**, 1704-1716.

Hermann, B. P., Sukhwani, M., Simorangkir, D. R., Chu, T. J., Plant, T. M. and Orwig, K. E. (2009b). Molecular dissection of the male germ cell lineage identifies putative spermatogonial stem cells in rhesus macaques. *Hum. Reprod.* **24**, 1704-1716.

Huckins, C. (1971). The spermatogonial stem cell population in adult rats. I. Their morphology, proliferation and maturation. *Anat. Rec.* **169**, 533-557.

Johnson, L. (1994). A new approach to study the architectural arrangement of spermatogenic stages revealed little evidence of a partial-wave along the length of human seminiferous tubules. *J. Androl.* **15**, 435-441.

Komai, Y., Tanaka, T., Tokuyama, Y., Yanai, H., Ohe, S., Omachi, T., Atsumi, N., Yoshida, N., Kumano, K., Hisha, H., et al. (2014). Bmi1 expression in long-term germ stem cells. *Sci. Rep.* **4**, 6175.

Lin, C. H., Yang, C. H. and Chen, Y. R. (2012). UTF1 deficiency promotes retinoic acid-induced neuronal differentiation in P19 embryonal carcinoma cells. *Int J Biochem Cell Biol* **44**, 350-357.

Lok, D. and de Rooij, D. G. (1983). Spermatogonial multiplication in the Chinese hamster. III. Labelling indices of undifferentiated spermatogonia throughout the cycle of the seminiferous epithelium. *Cell Tissue Kinet.* **16**, 31-40.

Lok, D., Jansen, M. T. and de Rooij, D. G. (1983). Spermatogonial multiplication in the Chinese hamster. II. Cell cycle properties of undifferentiated spermatogonia. *Cell Tissue Kinet.* **16**, 19-29.

Lok, D., Weenk, D. and de Rooij, D. G. (1982). Morphology, proliferation, and differentiation of undifferentiated spermatogonia in the Chinese hamster and the ram. *Anat. Rec.* **203**, 83-99.

Meng, X., Lindahl, M., Hyvonen, M. E., Parvinen, M., de Rooij, D. G., Hess, M. W., Raatikainen-Ahokas, A., Sainio, K., Rauvala, H., Lakso, M., et al. (2000). Regulation of cell fate decision of undifferentiated spermatogonia by GDNF. *Science* **287**, 1489-1493.

Muciaccia, B., Boitani, C., Berloco, B. P., Nudo, F., Spadetta, G., Stefanini, M., de Rooij, D. G. and Vicini, E. (2013). Novel stage classification of human spermatogenesis based on acrosome development. *Biol. Reprod.* **89**, 60, 61-10.

Neuhaus, N., Yoon, J., Terwort, N., Kliesch, S., Seggewiss, J., Huge, A., Voss, R., Schlatt, S., Grindberg, R. V. and Schöler, H. R. (2017). Single-cell gene expression analysis reveals diversity among human spermatogonia. *Mol Hum Reprod* **73**, 79-90.

Oatley, M. J., Kaucher, A. V., Racicot, K. E. and Oatley, J. M. (2011). Inhibitor of DNA binding 4 is expressed selectively by single spermatogonia in the male germline and regulates the self-renewal of spermatogonial stem cells in mice. *Biol. Reprod.* **85**, 347-356.

Rowley, M. J. and Heller, C. G. (1971). Quantitation of cells of seminiferous epithelium of human testis employing Sertoli cell as a constant. *Z Zellforsch Mikrosk Anat* **115**, 461-472.

Russell, L. D., Ettlin, R. A., Hikim, A. P. S. and Clegg, E. D. (1990). *Histological and histopathological evaluation of the testis*. Clearwater, Fl.: Cache River Press.

Scholzen, T. and Gerdes, J. (2000). The Ki-67 protein: from the known and the unknown. *J. Cell Physiol.* **182**, 311-322.

Schrans-Stassen, B. H., van de Kant, H. J., de Rooij, D. G. and van Pelt, A. M. (1999). Differential expression of c-kit in mouse undifferentiated and differentiating type A spermatogonia. *Endocrinology* **140**, 5894-5900.

Simorangkir, D. R., Marshall, G. R., Ehmcke, J., Schlatt, S. and Plant, T. M. (2005). Prepubertal expansion of dark and pale type A spermatogonia in the rhesus monkey (Macaca mulatta) results from proliferation during infantile and juvenile development in a relatively gonadotropin independent manner. *Biol Reprod* **73**, 1109-1115.

Simorangkir, D. R., Marshall, G. R. and Plant, T. M. (2009). A re-examination of proliferation and differentiation of type A spermatogonia in the adult rhesus monkey (Macaca mulatta). *Hum. Reprod.* **24**, 1596-1604.

Singh, D., Paduch, D. A., Schlegel, P. N., Orwig, K. E., Mielnik, A., Bolyakov, A. and Wright, W. W. (2017). The production of glial cell line-derived neurotrophic factor by human sertoli cells is substantially reduced in Sertoli cell-only testes. *Hum Reprod* **32**, 1106-1117.

Spinnler, K., Kohn, F. M., Schwarzer, U. and Mayerhofer, A. (2010). Glial cell line-derived neurotrophic factor is constitutively produced by human testicular peritubular cells and may contribute to the spermatogonial stem cell niche in man. *Human Reproduction* **25**, 2181-2187.

Tegelenbosch, R. A. and de Rooij, D. G. (1993). A quantitative study of spermatogonial multiplication and stem cell renewal in the C3H/101 F1 hybrid mouse. *Mutat. Res.* **290**, 193-200.

Tokunaga, Y., Imai, S., Torii, R. and Maeda, T. (1999a). Alterations of basal lamina of the seminiferous epithelium during the seasonal suppression of spermatogenesis in the Japanese monkey (Macaca fuscata). *Acta Histochemica Et Cytochemica* **32**, 359-368.

---- (1999b). Cytoplasmic liberation of protein gene product 9.5 during the seasonal regulation of spermatogenesis in the monkey (Macaca fuscata). *Endocrinology* **140**, 1875-1883.

van Alphen, M. M., van de Kant, H. J. and de Rooij, D. G. (1988). Depletion of the spermatogonia from the seminiferous epithelium of the rhesus monkey after X irradiation. *Radiat. Res.* **113**, 473-486.

van den Boom, V., Kooistra, S. M., Boesjes, M., Geverts, B., Houtsmuller, A. B., Monzen, K., Komuro, I., Essers, J., Drenth-Diephuis, L. J. and Eggen, B. J. (2007). UTF1 is a chromatin-associated protein involved in ES cell differentiation. *J. Cell Biol.* **178**, 913-924.

von Kopylow, K., Kirchhoff, C., Jezek, D., Schulze, W., Feig, C., Primig, M., Steinkraus, V. and Spiess, A. N. (2010). Screening for biomarkers of spermatogonia within the human testis: a whole genome approach. *Hum. Reprod.* **25**, 1104-1112.

von Kopylow, K., Staege, H., Spiess, A. N., Schulze, W., Will, H., Primig, M. and Kirchhoff, C. (2012). Differential marker protein expression specifies rarefaction zone-containing human A(dark) spermatogonia. *Reproduction* **143**, 45-57.

Wistuba, J., Schrod, A., Greve, B., Hodges, J. K., Aslam, H., Weinbauer, G. F. and Luetjens, C. M. (2003). Organization of seminiferous epithelium in primates: relationship to spermatogenic efficiency, phylogeny, and mating system. *Biol. Reprod.* **69**, 582-591.

Figures

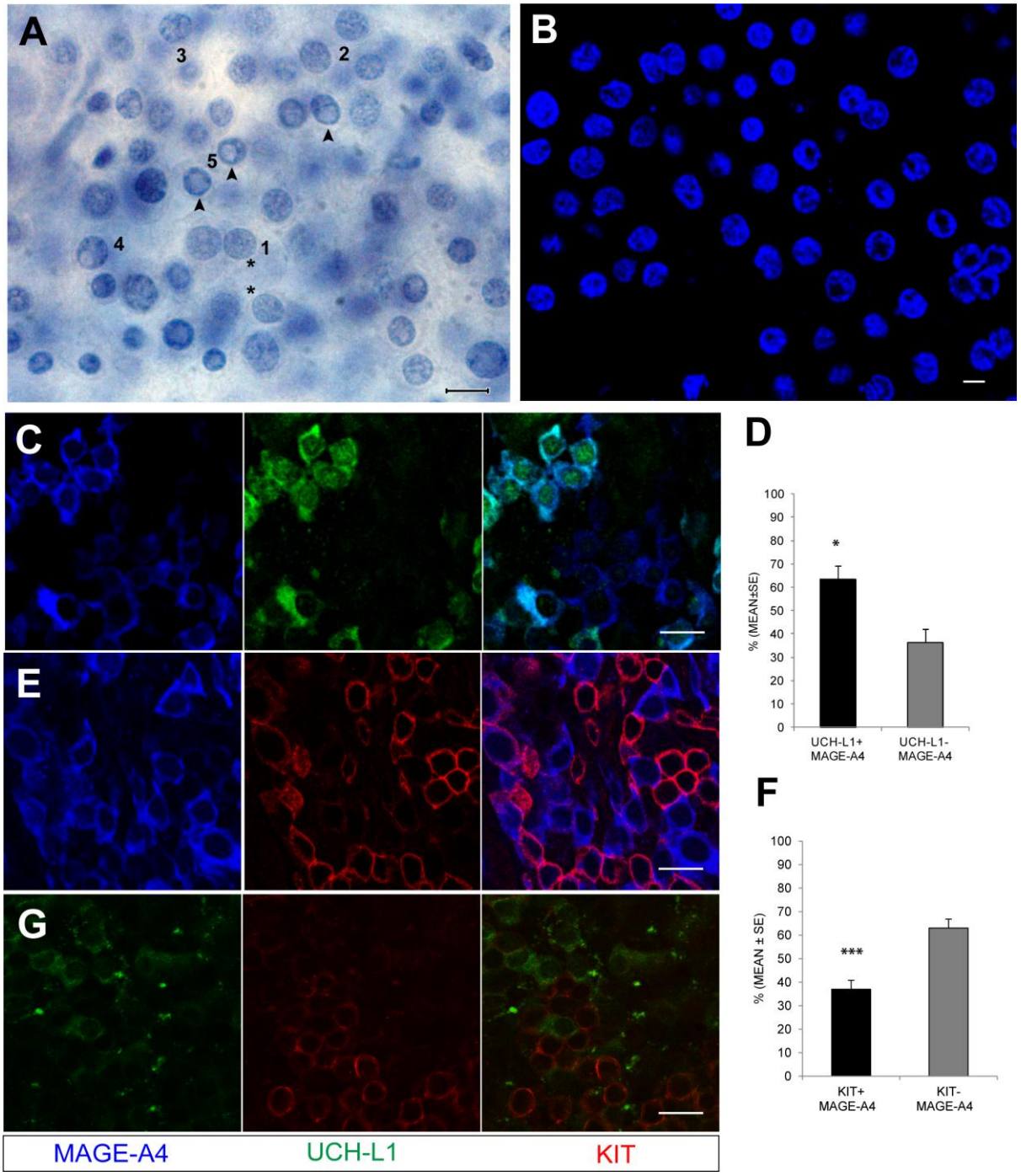

Fig. 1. Characterization of human spermatogonia. (A) View of the cells on the basal lamina of a human seminiferous tubule stained lightly with hematoxylin. Note the high density of spermatogonia and the variability of their morphology. Cells can be seen that are clear Ap (asterisk) and Ad (arrow heads) spermatogonia. However,

there are many nuclei with an intermediate morphology. Indeed, there may be a transition from Ap to Ad (follow the numbers 1 to 5). Intact seminiferous tubules were formalin-fixed and lightly stained with hematoxylin. Scale bar, 8 µm. **(B)** Cells on the basal lamina of an intact human seminiferous tubule stained with a fluorescent-dye for nuclear DNA. Note that no distinction can be made between Ap and Ad spermatogonia. Scale bar, 8 µm **(C,E,G)** Representative images of intact seminiferous tubules stained for UCH-L1 and MAGE-A4 **(C)**, MAGE-A4 and KIT (E), and UCH-L1 and KIT (G). Scale bar, 20 µm. **(D,F)** Quantification of the relative proportion of Ap-d (UCH-L1^{+}/MAGE-A4^{+}) and B (KIT^{+}/MAGE-A4^{+}) spermatogonia. **(D)** 1963 UCH-L1^{+}/MAGE-A4^{+} cells were scored in 3 samples. (F) 3315 KIT^{+}/MAGEA-A4^{+} cells were scored in 4 samples. *$p < 0.05$, ***$p < 0.001$ (Student's t- test).

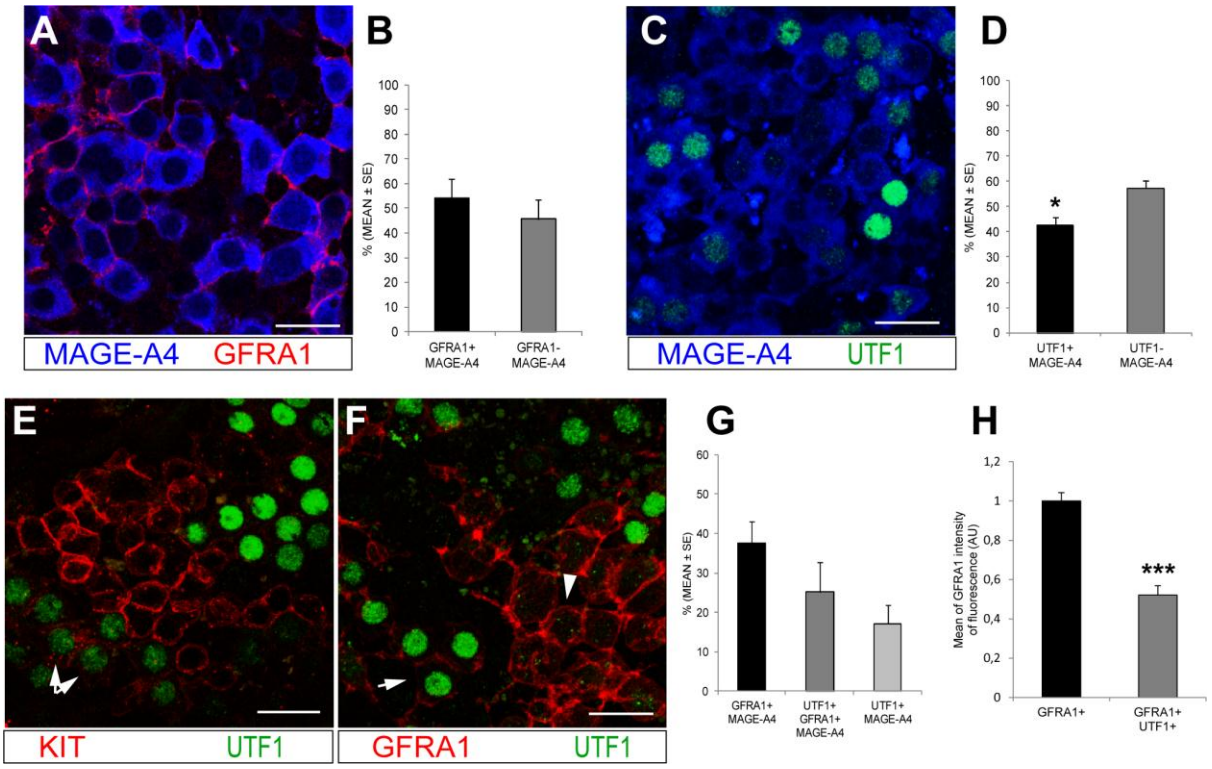

Fig. 2. Expression of GFRA1 and UTF1 in human spermatogonia. (A,B) Quantification of the relative proportion of GFRA1$^+$ and GFRA1$^-$ in human spermatogonia. **(A)** Representative images of intact seminiferous tubules co-stained for MAGE-A4 and GFRA1. **(B)** A total of 5850 GFRA1$^+$/MAGE-A4 and 5350 GFRA1$^-$ /MAGE-A4 cells were scored in 5 samples. **(C,D)** Quantification of the relative proportion of UTF1$^+$ and UTF1$^-$ in human spermatogonia. **(C)** Representative images of intact seminiferous tubules co-stained for MAGE-A4 and UTF1. **(D)** A total of 3316 UTF1$^+$/MAGE-A4 and 4463 UTF1$^-$/MAGE-A4 cells were scored in 3 samples. *$p < 0.05$ (Student's t- test). **(E)** Representative images of intact seminiferous tubules co-stained for KIT and UTF1. Double arrows: KIT$^+$/UTF1$^+$ positive spermatogonia. Note that KIT staining is weak in double-positive cells. **(F,G)** Quantification of the co-expression of GFRA1 and UTF1 among human spermatogonia. **(F)** Representative images of intact seminiferous tubules co-stained for MAGE-A4, GFRA1 and UTF1. Arrowhead: GFRA1$^+$/UTF1$^-$; arrow: GFRA1$^+$/UTF1$^+$. Note that GFRA1 expression level is higher in the GFRA1$^+$/UTF1$^-$ Ap-d spermatogonia. **(G)** A total of 1467 GFRA1$^+$, 684 UTF1$^+$ and 974 GFRA$^+$/UTF1$^+$ cells were scored in 3 samples **(H)** Data are from n=3 samples for a total of 240 cells analyzed. In each sample, 40

GFRA1/UTF1$^-$ Ap-d and 40 GFRA1/UTF1$^+$ Ap-d were analyzed. ***$p < 0.001$ (Student's t- test). Dashed lines: outline of the seminiferous tubules. Scale bars, 20 µm.

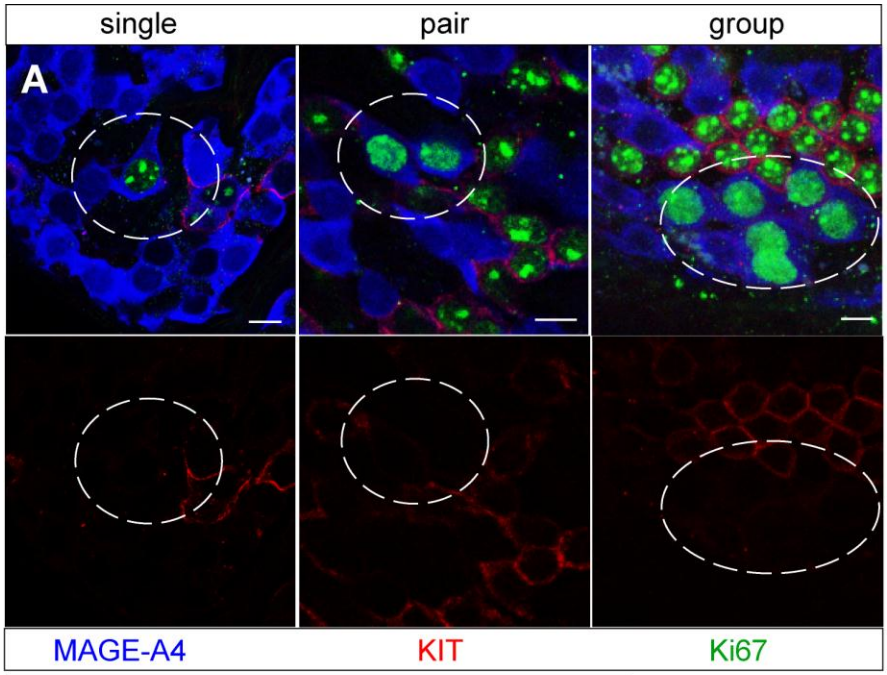

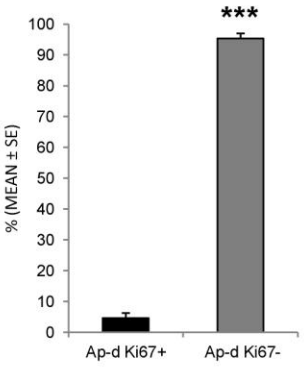

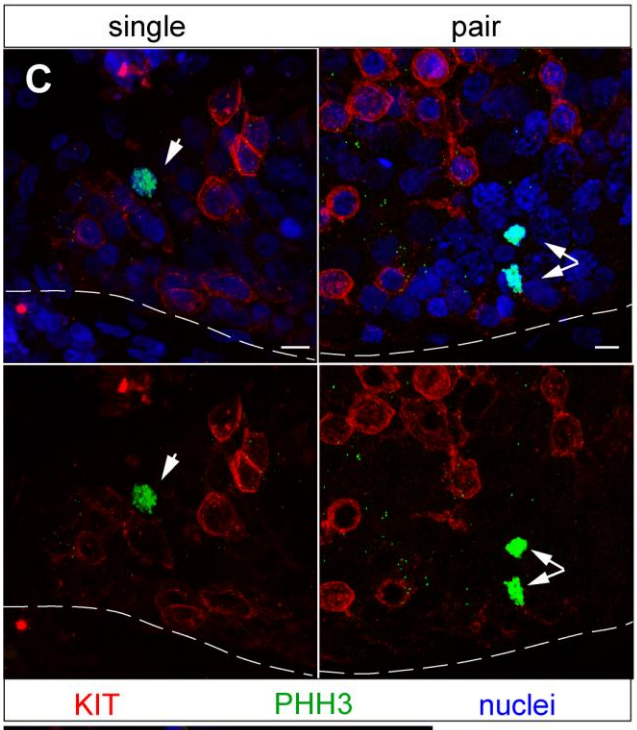

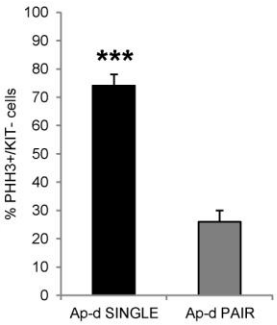

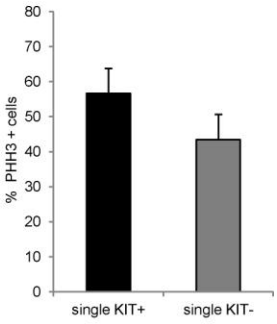

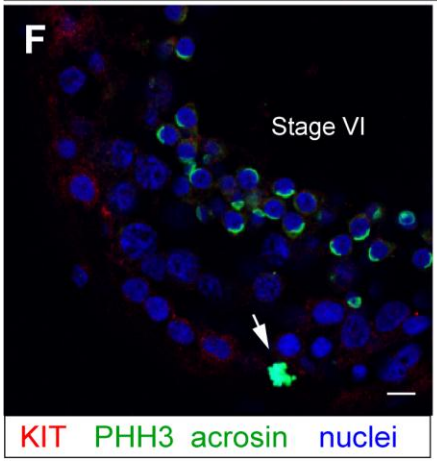

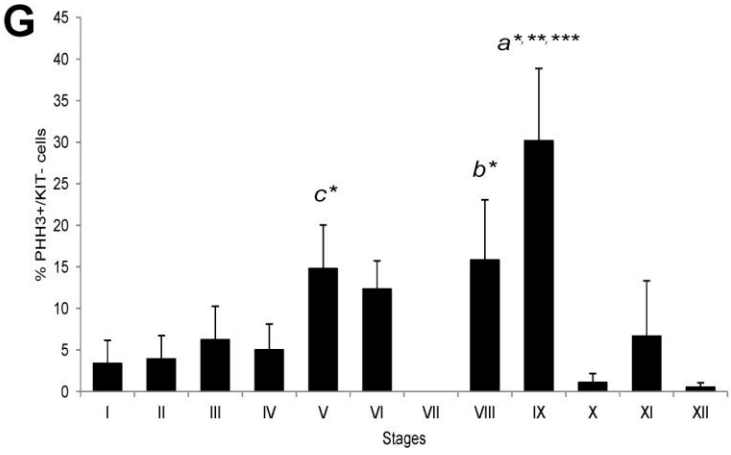

Fig. 3. Kinetics of human Ap-d spermatogonia. (A,B) Proliferation index of Ap-d. **(A)** Representative images of intact seminiferous tubules co-stained for KI67 to detect proliferating cells, MAGE-A4 and KIT. Dashed circles show a single (left), a pair (center) and a group (right) of $KI67^+$ Ap-d ($MAGE\text{-}A4^+/KIT^-$). **(B)** Quantification of proliferation index in 3 samples. A total of 102 $KI67^+$ Ap-d were scored out of 2235 Ap-d. ***p < 0.001 (Student's t- test). **(C,D)** Quantification of the relative proportion of single and pair Ap-d ($KIT^-/MAGE\text{-}A4^+/PHH3^+$). **(C)** Representative images of intact seminiferous tubules co-stained for PHH3 to detect mitotic spermatogonia, MAGE-A4 and for KIT. Single arrow: single Ap-d; double arrow: paired Ap-d. Dashed lines: outline of the seminiferous tubules. **(D)** Relative proportion of single and pair Ap-d and 12 KIT^- pairs were scored in 5 samples. ***p<0.001, (Student's t- test). **(E)** Quantification of the relative proportion of single Ap-d ($KIT^-/MAGE\text{-}A4^+/PHH3^+$) and single B ($KIT^+/MAGE\text{-}A4^+/PHH3^+$) spermatogonia. A total of 37 KIT^- and 55 KIT^+ single cells were scored in 5 samples. **(F,G)** Distribution of mitotic Ap-d during the cycle of the seminiferous epithelium. **(F)** Representative images of formalin-fixed testis section stained for PHH3 to detect mitotic cells, KIT a marker of B spermatogonia and acrosin to visualize the epithelial stage. Nuclei are stained with TO-PRO-3. Single arrow: mitotic Ap-d at stage VI. **(G)** Histogram showing percentage of mitotic Ap-d ($PHH3^+/KIT^-$) per stage. A total of 64 $PHH3^+/KIT^-$ spermatogonia were counted in 6 samples. a*: p<0.05 stage IX versus stage V,VI and VIII; a**: p< 0.005 stage IX versus III and XI; a***: p<0.001 stage IX versus I, II, IV, X, XII; b*: p<0.05 stage VIII versus X and XII; c*: p<0.05 stage V versus X and XII. Scale bars, 10 µm

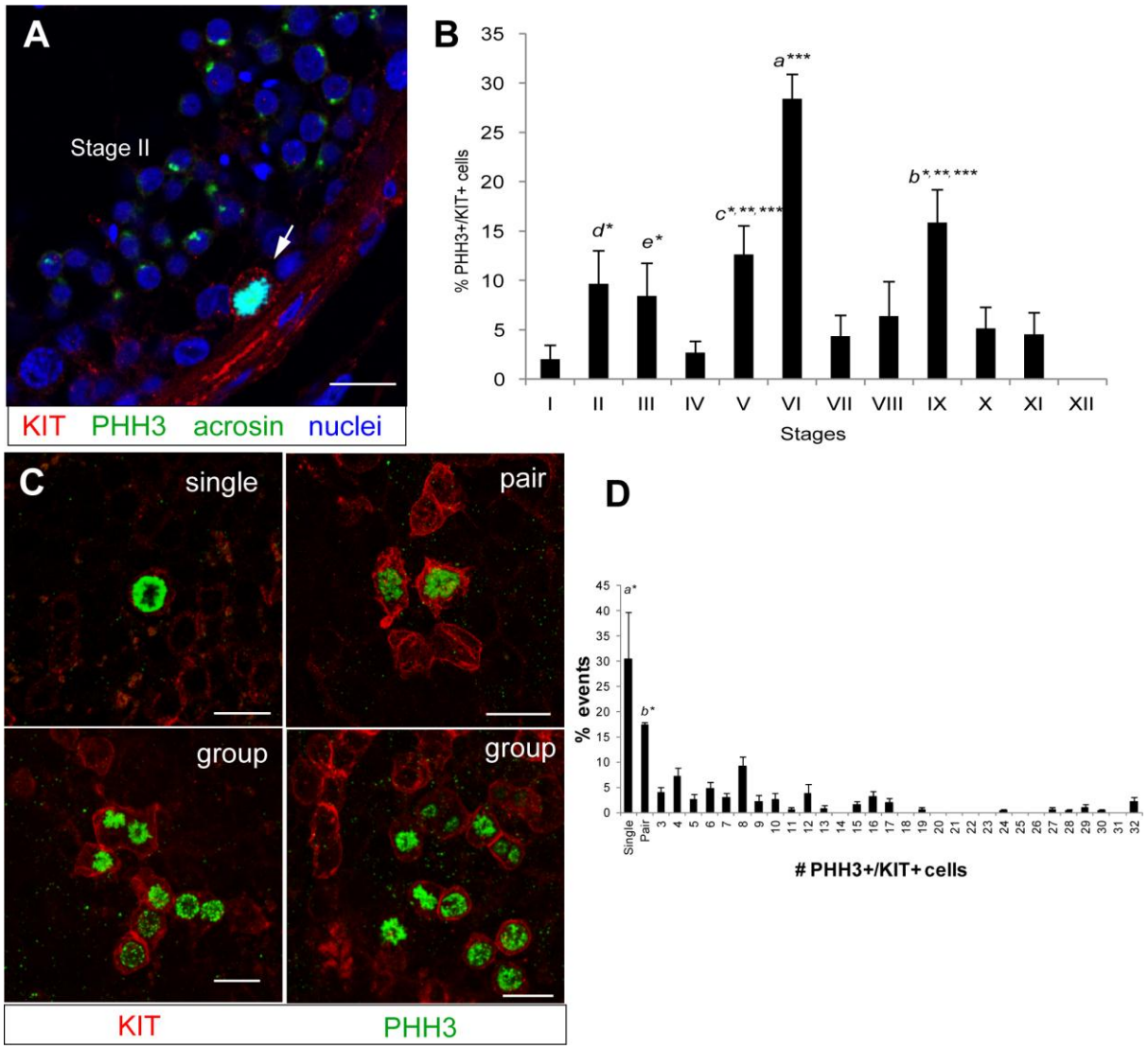

Fig. 4. Kinetics of human B spermatogonia. (A,B) Distribution of mitotic B spermatogonia during the cycle of the seminiferous epithelium. **(A)** Representative images of formalin-fixed testis sections stained for PHH3, KIT and acrosin to visualize the epithelial stage. Nuclei were stained with TO-PRO-3. Single arrow: mitotic B spermatogonia at stage II. **(B)** Histogram showing the percentage of mitotic B spermatogonia ($PHH3^+/KIT^+$) per stage. A total of 260 $PHH3^+/KIT^+$ spermatogonia were counted in 6 samples. a***: p<0.001 stage VI versus all other stages; b***: p<0.001 stage IX versus stages I,IV and XII; b**: p<0.005 stage IX versus stages VII,X and XI; b* p<0.05 stage IX versus stages III and VIII; c***: p<0.001 stage V versus stage XII; c**: p=0.05 stage V versus stage I; c*: p< 0.05 stage V versus stages IV,VII,X and XI; d*: p<0.05 stage II versus stages I and XII; e*: p<0.05 stage III versus stage XII. **(C,D)** Topographical arrangement of clones of mitotic B

spermatogonia. **(C)** Intact seminiferous tubules co-stained for PHH3 and KIT. Representative images of singles, pairs and groups of $PHH3^+$ B spermatogonia. **(D)** Relative frequencies of singles, pairs and groups of 3 up to 32 mitotic B spermatogonia in intact seminiferous tubules. A total of 260 $PHH3^+/KIT^+$ cells were scored in 6 samples. a*: $p<0.05$ single versus all others except pair; b*:$p<0.05$ pair versus all others except single. Scale bars, 20 µm.

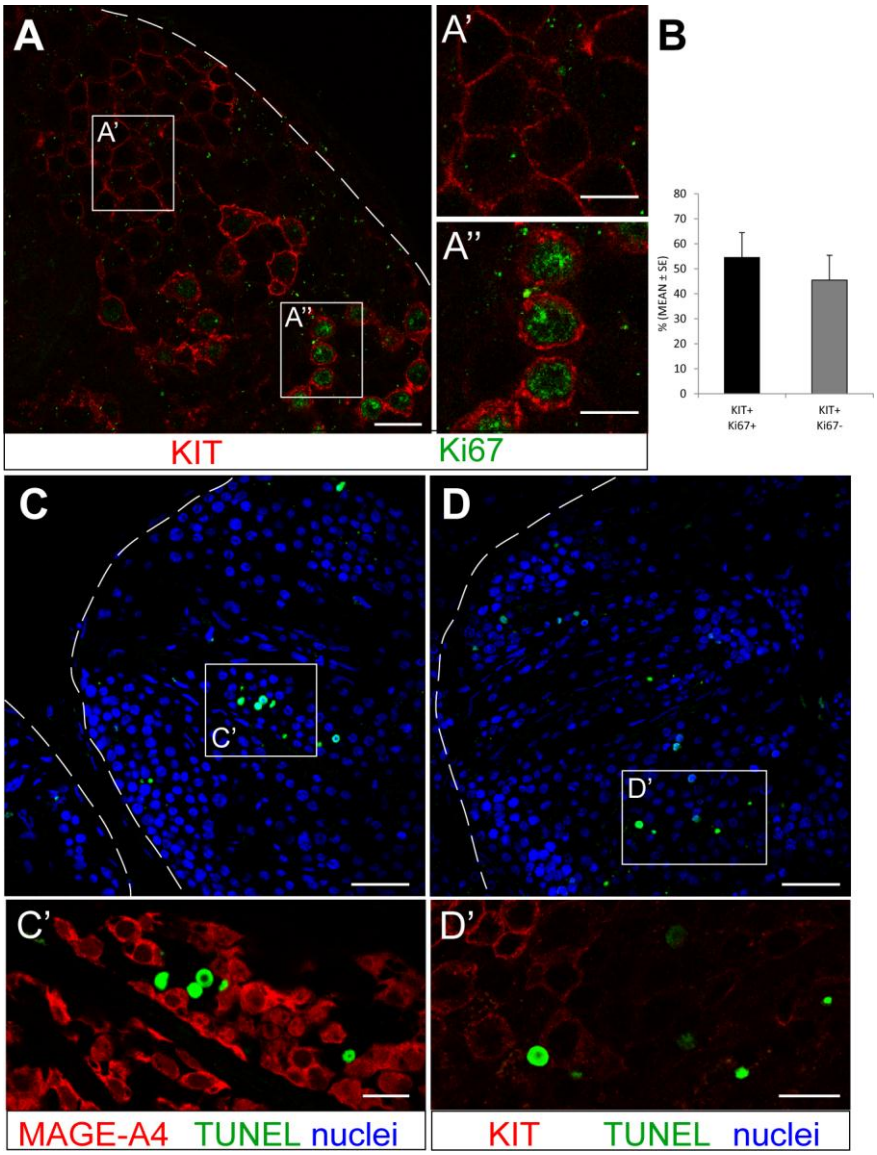

Fig. 5. Regulation of human differentiating spermatogonia. (A,B) Proliferation index of B spermatogonia. **(A)** Representative images of intact seminiferous tubules co-stained for KI67 and KIT. **(B)** A total of 742 $Ki67^{+}/KIT^{+}$ and 633 $Ki67^{-}/KIT^{+}$ cells were scored in 3 samples. **(C,D)** TUNEL assay on human human seminiferous tubules. **(C)** Representative images of intact seminiferous tubules co-stained for TUNEL, MAGE-A4 and TO-PRO-3. An enlargement of the boxed area is shown in C'. **(D)** Representative images of intact seminiferous tubules co-stained for TUNEL, KIT and TO-PRO-3. An enlargement of the boxed area is shown in D'. Dashed lines: outline of the seminiferous tubules. Scale bars: 10 μm in A' and A''; 20 μm in A C' and D'; 50 μm in C and D.

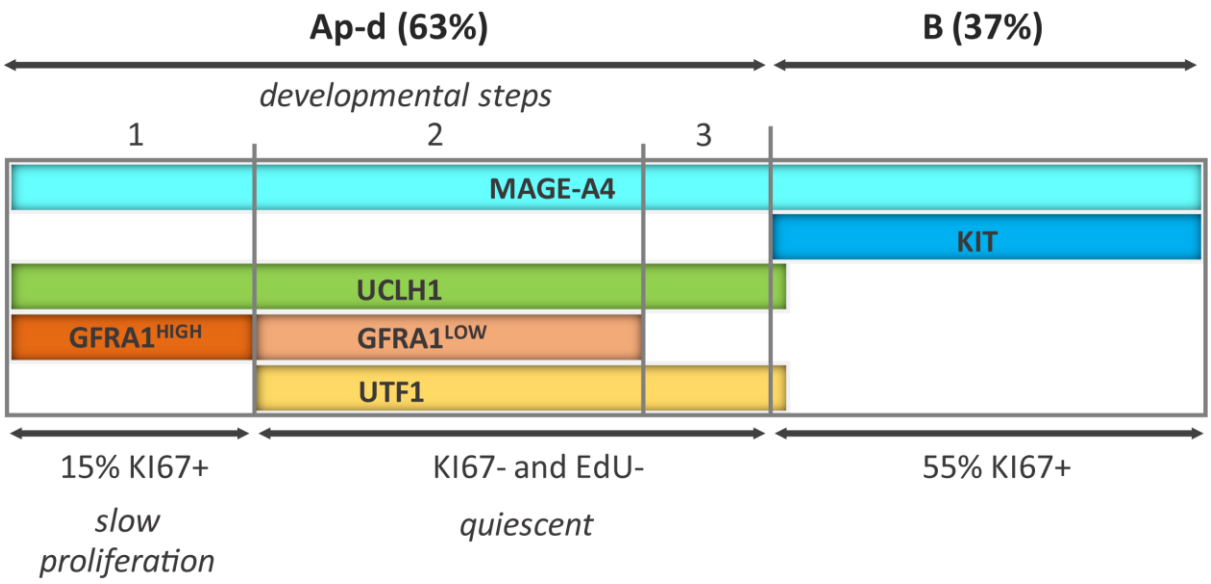

Fig. 6. Proposed scheme for human spermatogonial multiplication and stem cell renewal, based on marker protein expression and mitotic activity of the cells. The SSCs reside in the GFRA1^{High}/UTF1^{-} Ap-d spermatogonia and differentiating cells are recruited from GFRA1^{Low}/UTF1^{+} Ap-d spermatogonia. Note the very low proliferative activity of the Ap-d.

Figure S1. Sertoli cell nuclei are localized in the second layer of cells above the basal lamina. Related to Figure 1

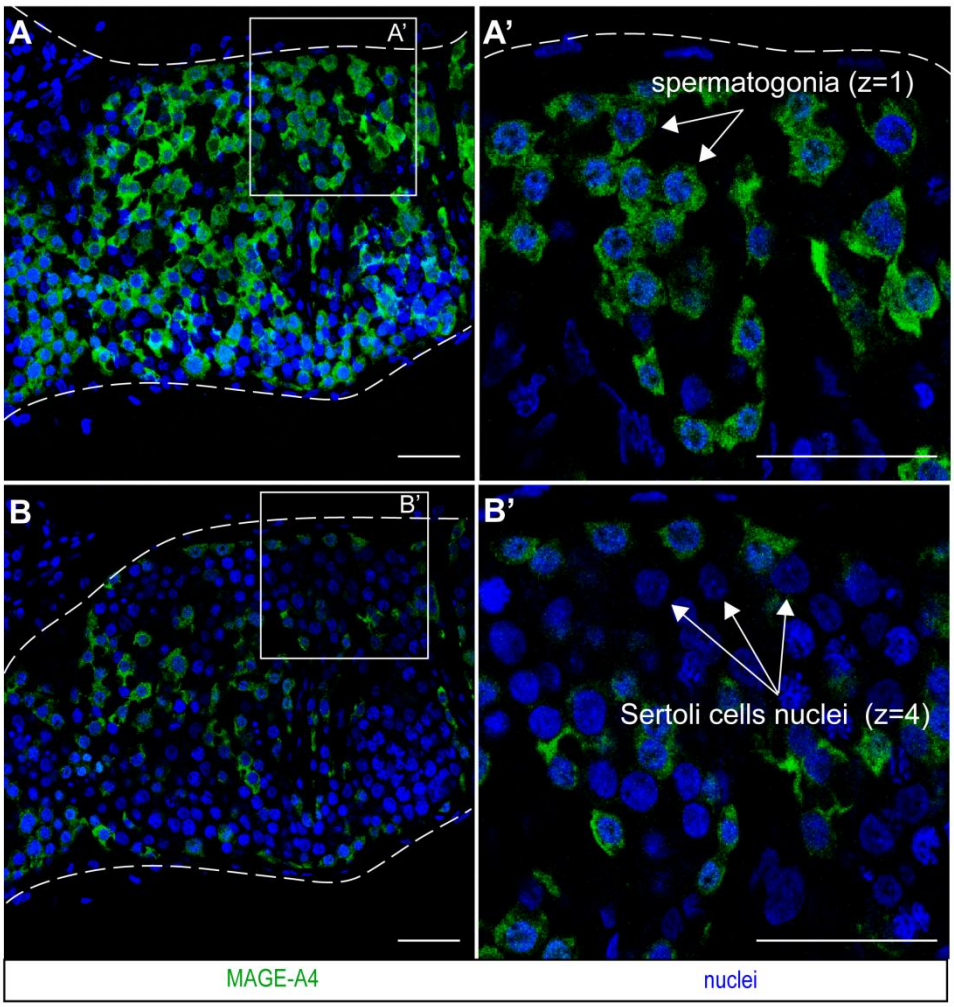

Figure S1. Sertoli cell nuclei are localized in the second layer of cells above the basal lamina (see Figure 1). (A,B) Intact seminiferous tubules were stained with MAGE-A4 and TO-PRO-3 to detect nuclei. Tubules were scanned with a confocal microscope from the basal lamina layer z=1 (A) to the Sertoli cell layer z=4 (B). Boxed regions in A and B are shown enlarged in A' and B', respectively. Spermatogonia were recognized by MAGE-A4 staining, while Sertoli cell were recognized by their typical nuclear morphology. Scale bars, 50 μm

Figure S2. Markers analysis in S-phase preleptotene spermatocytes. Related to Figure 1.

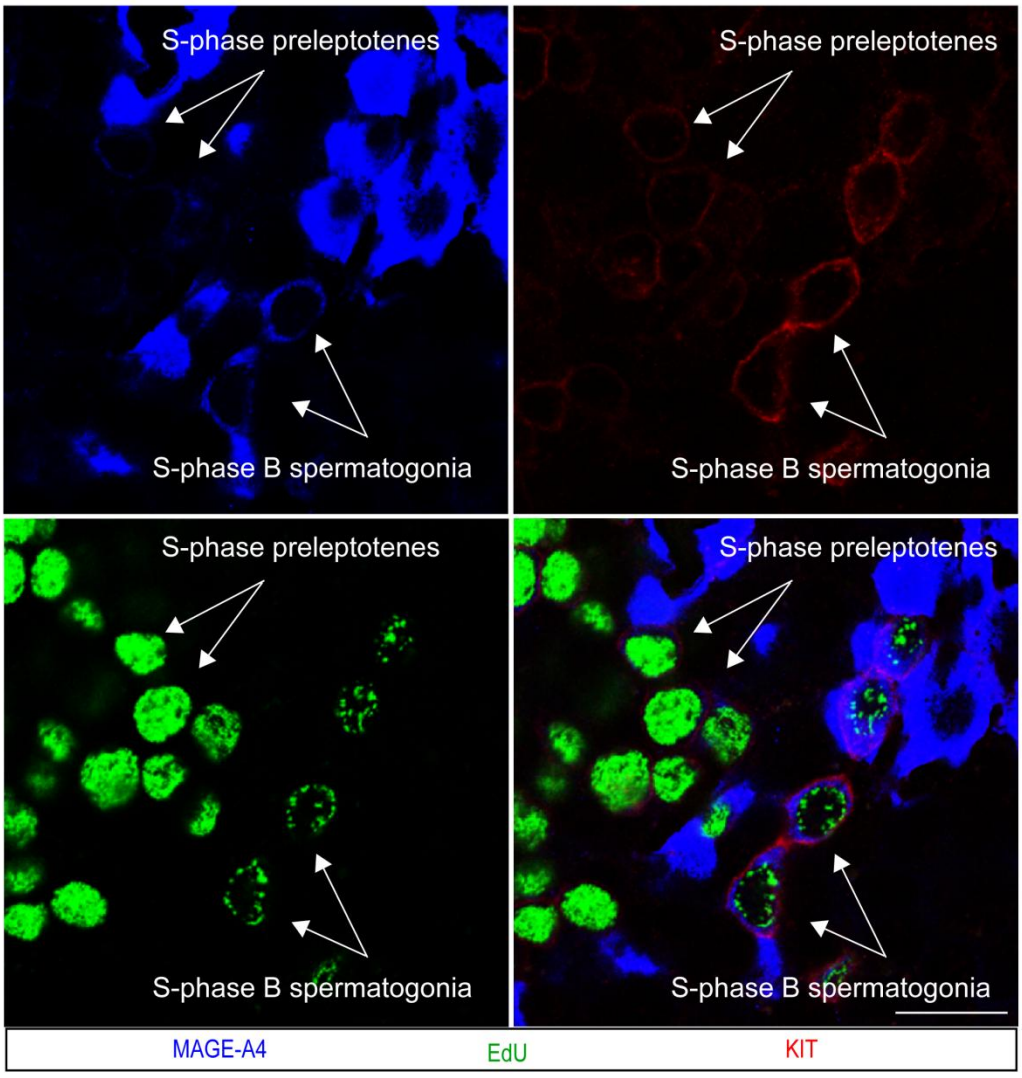

Figure S2. Markers analysis in S-phase preleptotene spermatocytes (see Figure1). Intact seminiferous tubules were shortly cultured in the presence of EdU to label cells in S-phase of the cycle. At the end seminiferous tubule were stained to detect EdU, KIT and MAGE-A4. Note that S-phase preleptotene spermatocytes are MAGE-A4^{-} and KIT$^{low.}$ Scale bar, 20 µm.

Figure S3. Proliferation index of GFRA1^{+} Ap-d. Related to Figure 2.

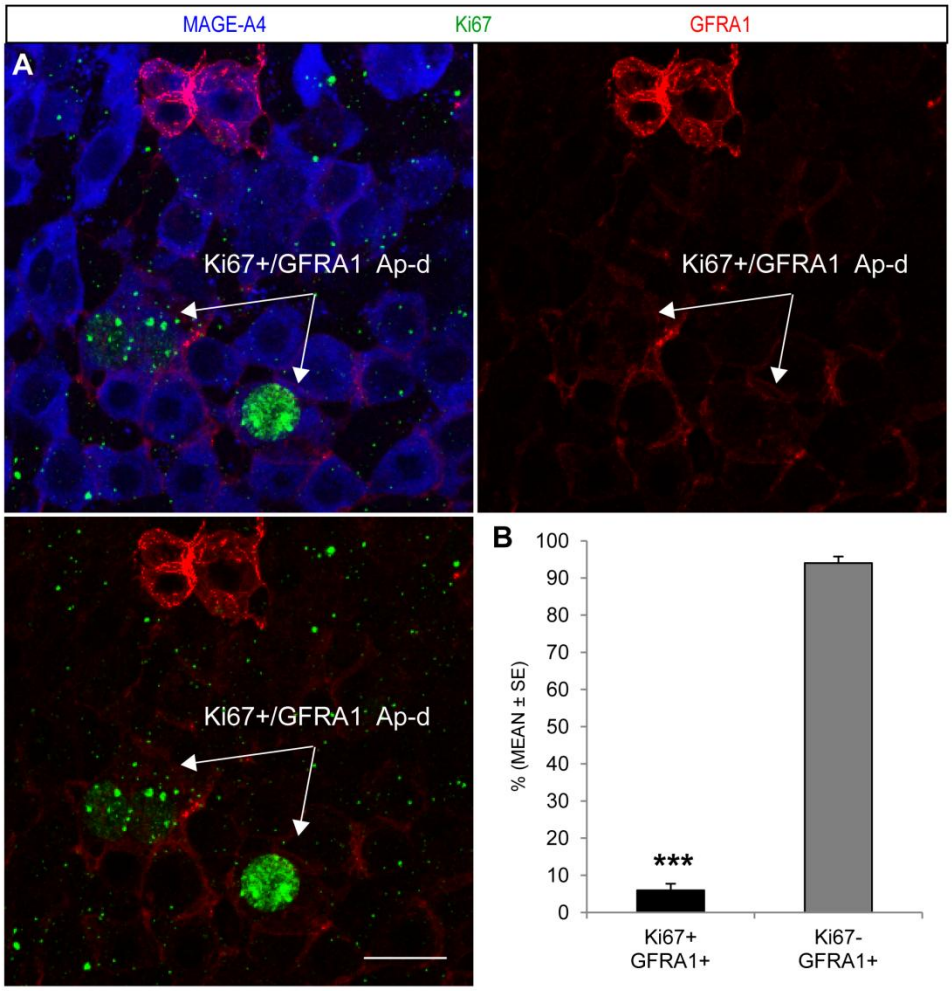

Figure S3. Proliferation index of GFRA1 Ap-d (see figure 2). (A) Representative images of intact seminiferous tubules co-stained for Ki67 to detect proliferating cells, MAGE-A4 a marker of all spermatogonia and GFRA1, a marker of Ap-d spermatogonia. Double arrow indicate Ki67^{+}/GFRA1^{+} Ap-d. (B) Quantification of proliferation index. Error bars, mean ± SEM, n=4 samples. A total of 142 Ki67^{+} Ap-d were scored out of 2491 MAGE-A4^{+}/GFRA1^{+} cells. ***p < 0.001 (Student's t- test). Scale bar, 20 μm.

Figure S4. Murine differentiating spermatogonia are all engaged in the cell cycle. Related to Figure 5.

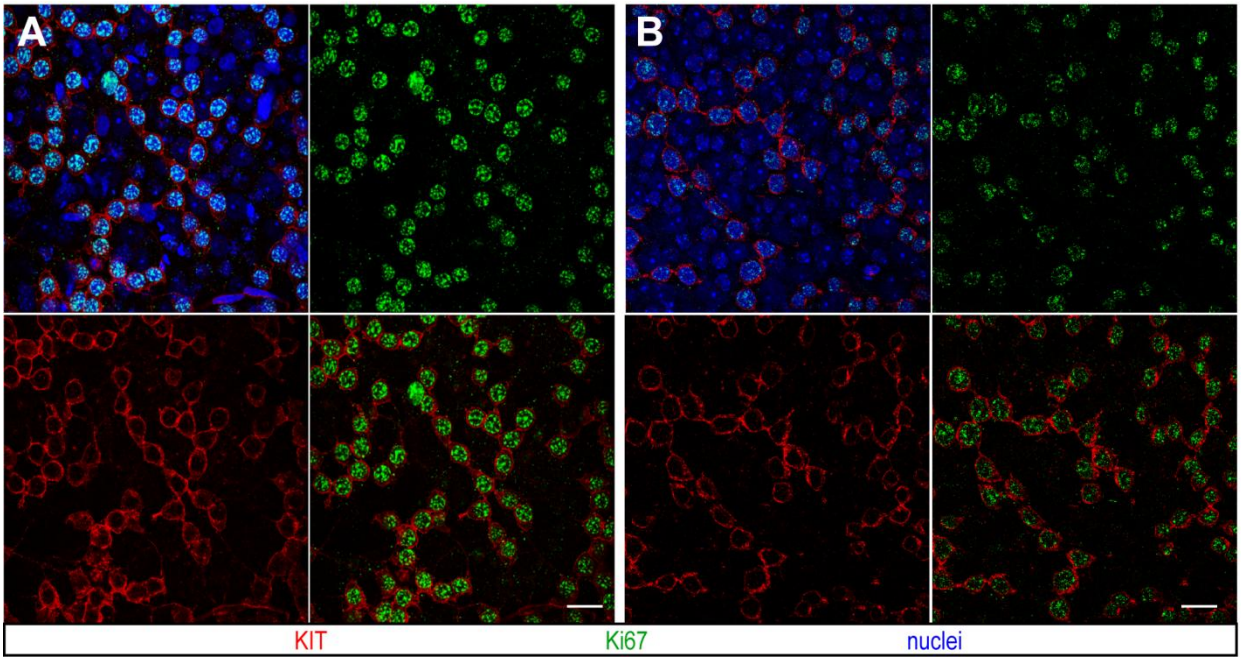

Figure S4. Murine differentiating spermatogonia are all engaged in the cell cycle (see Figure 5). (A,B) Representative images of intact murine seminiferous tubules co-stained for Ki67, to detect proliferating cells and KIT a marker of differentiating spermatogonia. Note that all the KIT^{+} spermatogonia are $KI67^{+}$. Scale bars, 20 µm.

Table S1. Antibodies

Antibody	Species	Dilution	Company	City	Country
UTF1	Mouse	1:50	Millipore MAB4337	Milan	Italy
GFRA1	Goat	1:25	R&D AF714	Milan	Italy
Acrosin	Mouse	1:1000	Biosonda Biotechnology Acr-C5GF10	Santiago	Chile
PHH3	Rabbit	1:200	Merck 06570	Milan	Italy
KIT	Goat	1:25	R&D AF332	Milan	Italy
KIT	Goat	1:50	R&D AF1356	Milan	Italy
MAGE-A4	Mouse	1:100	Gift from G. Spagnoli		
KI67	Rabbit	1:200	Abcam AB15580	Cambridge	UK

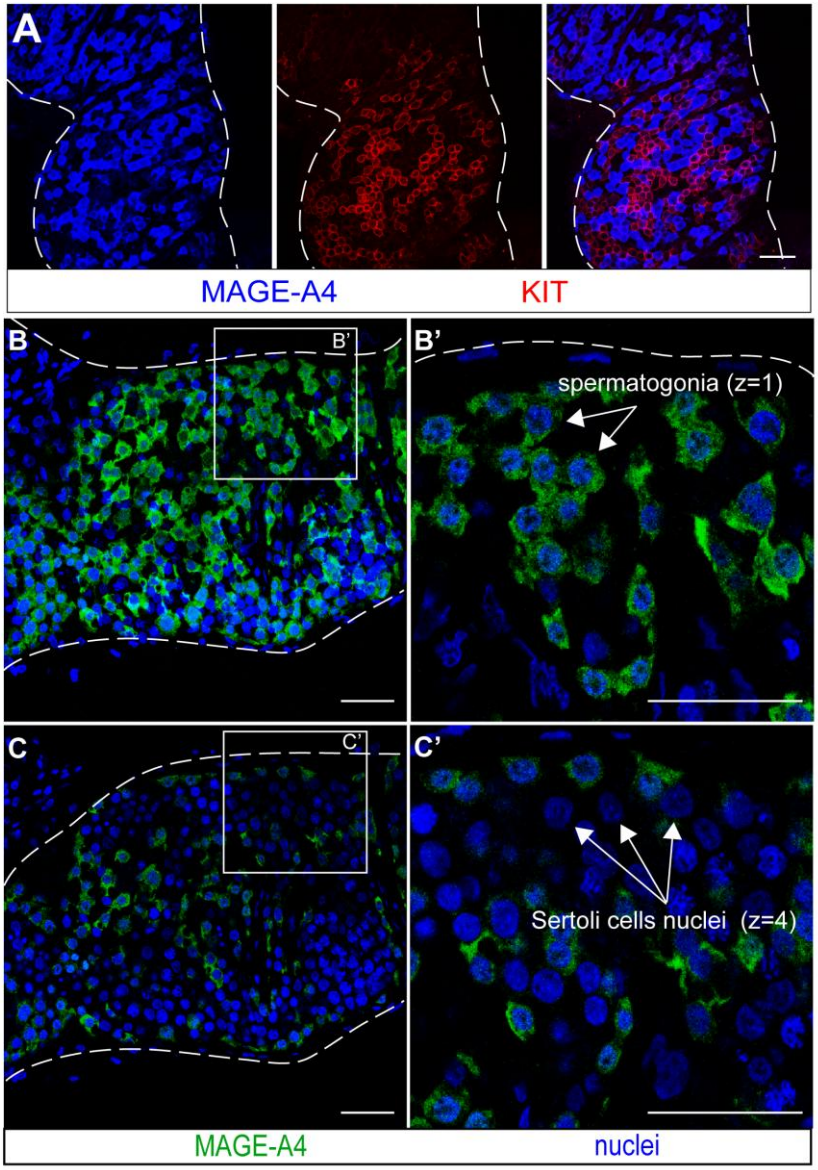

Figure S1. Sertoli cell nuclei are localized in the second layer of cells above the basal lamina (see Figure 1). **(A)** Representative images of intact seminiferous tubules stained for MAGE-A4, a marker of all spermatogonia, and KIT, a marker of B spermatogonia. Dashed lines: outline of the seminiferous tubules. Scale bar, 50 μm. **(B, C)** Intact seminiferous tubules were stained with MAGE-A4 and TO-PRO-3 to detect nuclei. Tubules were scanned with a confocal microscope from the basal lamina layer z=1 (B) to the Sertoli cell layer z=4 **(C)**. Boxed regions in B and C are shown enlarged in B' and C', respectively. Spermatogonia were recognized by MAGE-A4 staining, while Sertoli cells were recognized by the typical nuclear morphology. Scale bars, 50 μm.

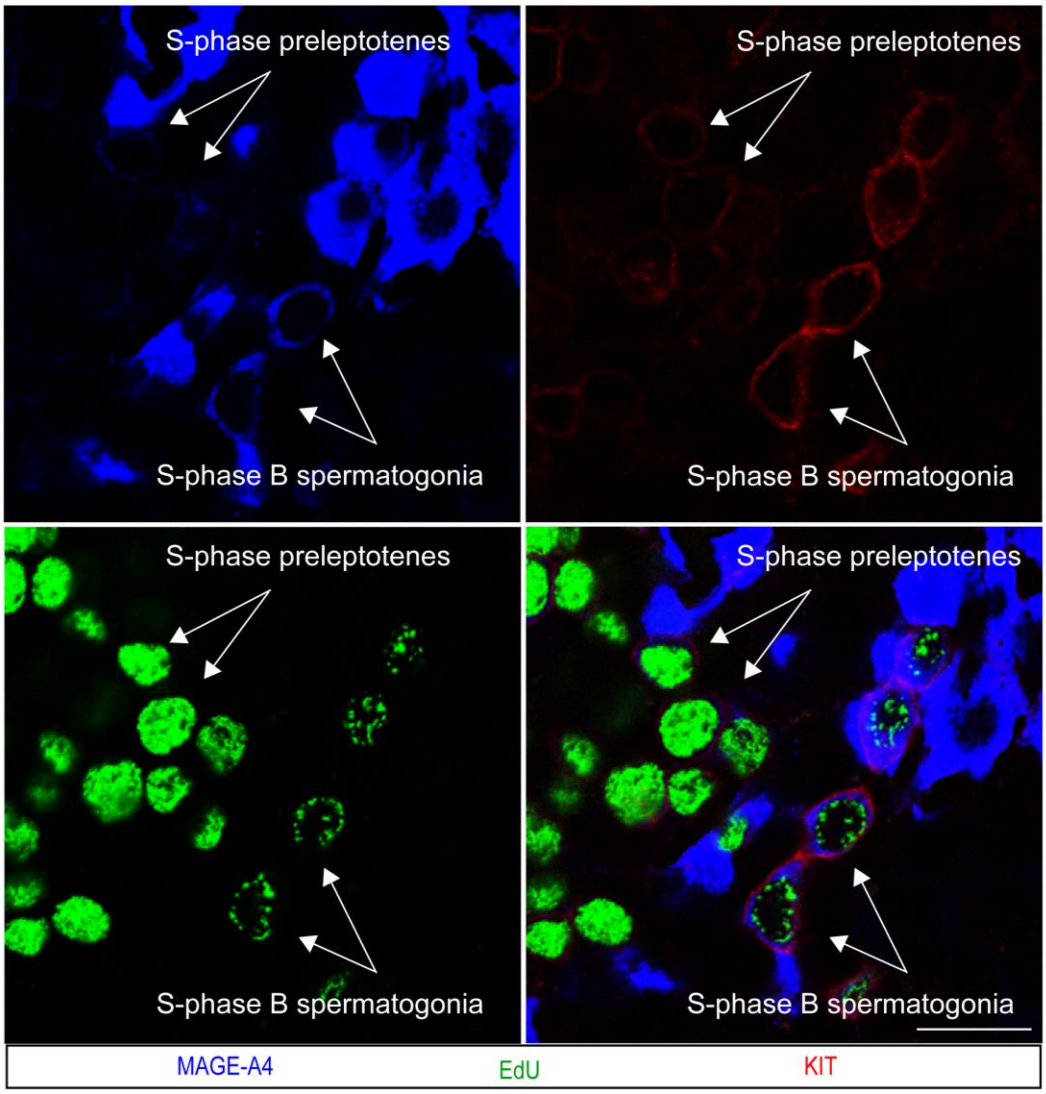

Fig. S2. Markers analysis in preleptotene spermatocytes in S-phase (see Figure 1). Intact seminiferous tubules were shortly cultured in the presence of EdU to label cells in S-phase of the cycle. At the end, seminiferous tubules were stained to detect EdU, KIT and MAGE-A4. Note that S-phase preleptotene spermatocytes are MAGE-A4 $^{-}$ and KIT^{low}. Scale bar, 20 μm.

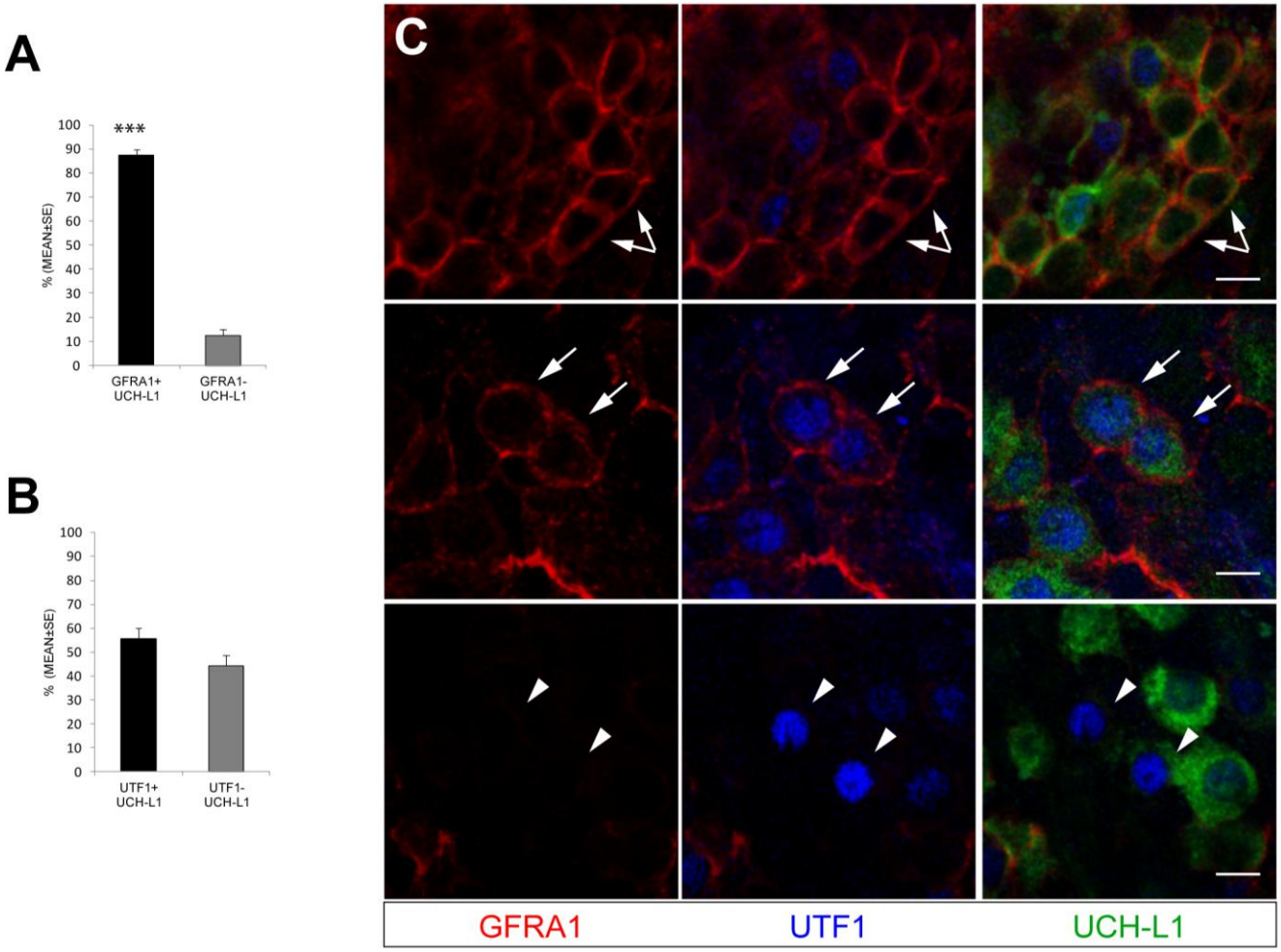

Fig. S3 Expression of UCHL1, GFRA1 and UTF1 in human spermatogonia. Related to Figure 2. (A) Quantification of GFRA1+ proportion in Ap-d spermatogonia. A total of 1301 GFRA1$^+$/UCH-L1 cells were scored in 3 samples. **(B)** Quantification of UTF1$^+$ cells among Ap-d spermatogonia. A total of 798 UTF1$^+$/UCH-L1 cells were scored in 3 samples. **(C)** Representative images of intact seminiferous tubules co-stained for UCH-L1, GFRA1 and UTF1. Double arrow indicate GFRA1$^+$/UCH-L1$^+$ Ap-d, arrows indicate GFRA1$^+$/UTF1$^+$/UCH-L1$^+$ Ap-d, arrowheads indicate UTF1$^+$/UCH-L1$^+$ Ap-d. ***$p < 0.001$ (Student's t- test).

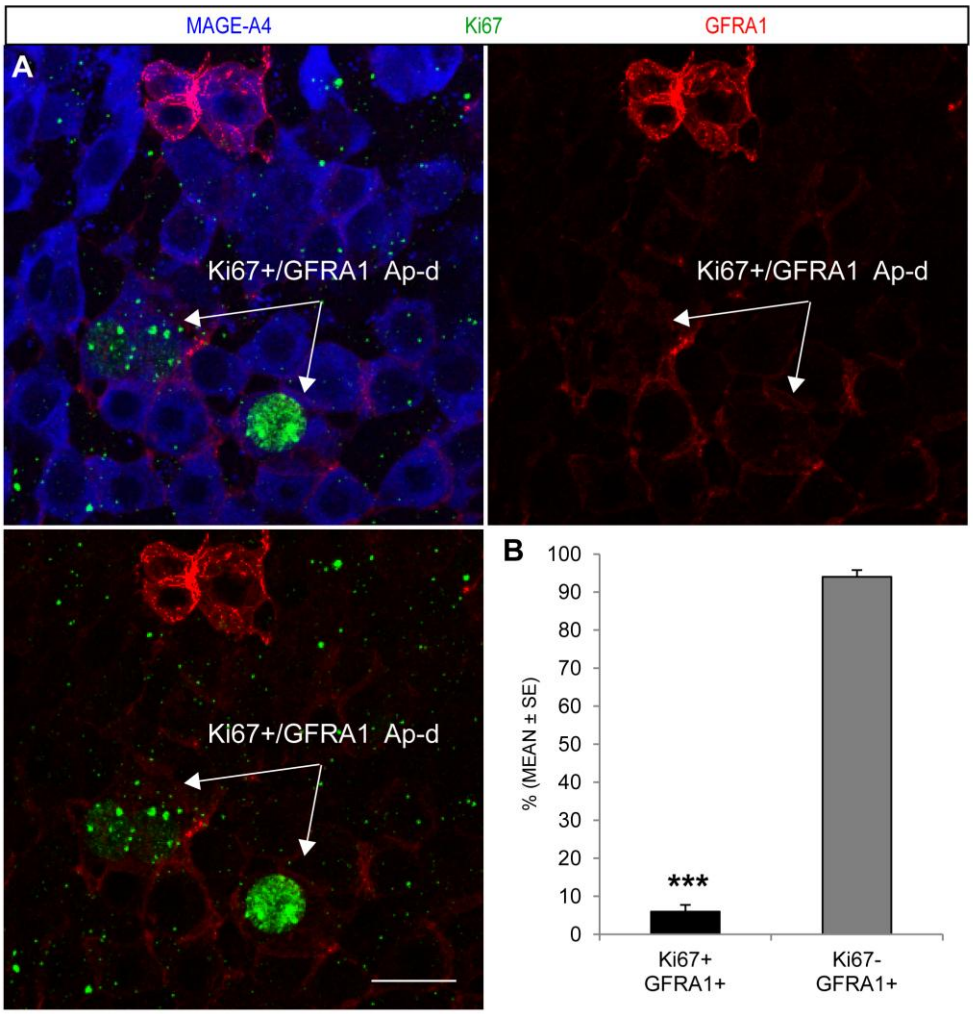

Fig. S4. Proliferation index of GFRA1$^+$ Ap-d (see Figure 3). (A) Representative images of intact seminiferous tubules co-stained for Ki67, to detect proliferating cells, MAGE-A4 a marker of all spermatogonia and GFRA1, a marker of Ap-d spermatogonia. Double arrow indicate KI67$^+$/GFRA1$^+$ Ap-d. **(B)** Quantification of proliferation index. Error bars, mean ± SEM, n=4 samples. A total of 142 KI67$^+$ Ap-d were scored out of 2491 MAGE-A4$^+$/GFRA1$^+$ cells. ***<0.001 (Student's t-test). Scale bar, 20 μm.

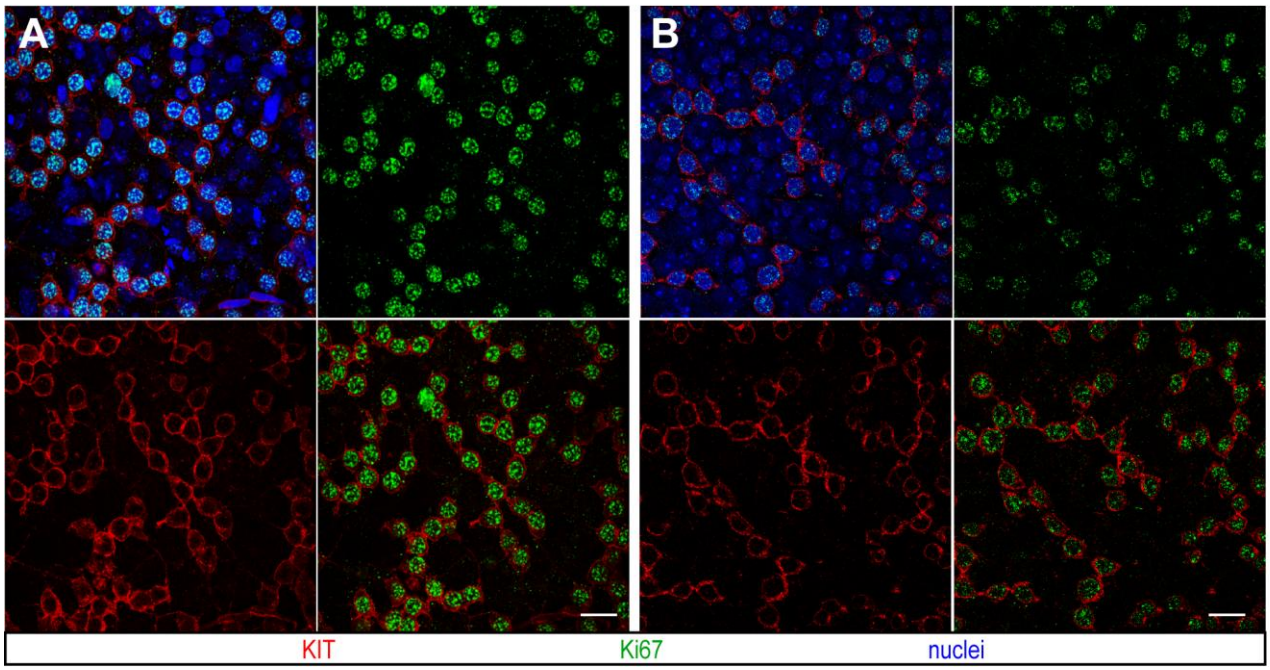

Figure S5. Murine differentiating spermatogonia are all engaged in the cell cycle. Related to Figure 5.
(A,B) Representative images of intact murine seminiferous tubules co-stained for Ki67, to detect proliferating cells and KIT, a marker of differentiating spermatogonia. Note that all the KIT^{+} spermatogonia are $Ki67^{+}$. Scale bars, 20 μm.

Table S1. Antibodies

Antibody	Species	Dilution	Company	City	Country
UTF1	Mouse	1:50	Millipore MAB4337	Milan	Italy
GFRA1	Goat	1:25	R&D AF714	Milan	Italy
Acrosin	Mouse	1:1000	Biosonda Biotechnology Acr-C5GF10	Santiago	Chile
PHH3	Rabbit	1:200	Merck 06570	Milan	Italy
KIT	Goat	1:25	R&D AF332	Milan	Italy
KIT	Goat	1:50	R&D AF1356	Milan	Italy
MAGE-A4	Mouse	1:100	Gift from G. Spagnoli		
PGP 9.5 (UCH-L1)	Rabbit	1:100	Dako Z5116	Milan	Italy
KI67	Rabbit	1:200	Abcam AB15580	Cambridge	UK